This is a preprint, the final version is subject to change, of the American Mineralogist (MSA)
Cite as Authors (Year) Title. American Mineralogist, in press.
(DOI will not work until issue is live.) DOI: http://dx.doi.org/10.2138/am-2017-5918

REVISION 1

Tightly bound water in smectites

Authors: Artur Kuligiewicz*, Arkadiusz Derkowski#

Institute of Geological Sciences, Polish Academy of Sciences, Senacka 1, PL31002 Krakow, Poland

* corresponding author e-mail: ndkuligi@cyf-kr.edu.pl

corresponding author e-mail: ndderkow@cyf-kr.edu.pl

This is a preprint, the final version is subject to change, of the American Mineralogist (MSA)
Cite as Authors (Year) Title. American Mineralogist, in press.
(DOI will not work until issue is live.) DOI: http://dx.doi.org/10.2138/am-2017-5918

Abstract

Smectites are able to retain molecular tightly bound water (TBW) at temperatures above 100 °C, even after prolonged drying. The presence of TBW affects the stable isotope ratios, the dehydroxylation behavior of smectites and smectite-rich samples and also has implications in measuring various properties of clay-rich rocks. Five reference smectites, in Mg-, Ca-, Na-, and Cs-exchanged forms were subjected to different drying protocols followed by the determination of TBW contents using precise thermogravimetric (TG) analysis. Activation energies (E_a) of the removal of different water fractions at temperatures up to 1000 °C were determined in non-isothermal TG experiments using model-independent methods. Additionally, 4A and 13X zeolites were examined in both cases as apparent OH-free references.

After drying at 110 °C all smectites still contained up to 3 water molecules per interlayer cation. The TBW contents in smectites were found to be primarily dependent on the isothermal drying temperature. For a given temperature, TBW contents decreased with respect to the type of interlayer cation in the following order: Mg>Ca>Na>Cs. The influence of the time of drying and the smectite layer charge were found to be negligible. The E_a of dehydration below 100 °C, as determined by the Friedman method, was quite constant within the 45-60 kJ/mol range. The E_a of TBW removal increased along with the degree of reaction from 90 to 180 kJ/mol, while the E_a of dehydroxylation was found in the 159-249 kJ/mol range, highly depending on the sample's octahedral sheet structure and the interlayer cation. The Mg^{2+} cation can hold H_2O molecules even beyond 550 °C, making it available during dehydroxylation or - for geologic-scale reactions – pass H_2O to metamorphic conditions.

High similarities between the TBW contents and the E_a of dehydration for smectites and cationic (low Si/Al-) zeolites lead to the conclusion that TBW in smectites is remarkably similar

to zeolitic water in terms of cation bonding and diffusion characteristics. The optimal drying protocol for smectites is to substitute interlayer cations with cations of a low hydration enthalpy, such as Cs, and to dry a sample at 300 °C, provided that the sample is Fe-poor. Fe-rich smectites should be dried at 200 °C to avoid dehydroxylation that occurs below 300 °C.

KEYWORDS: smectite, thermogravimetry, clay-bound water, dehydration, activation energy,

Introduction

Drying a rock, sediment, or soil sample is one of the most common and basic procedures in geoscience studies and in geotechnical applications. Prolonged heating of a sample at a temperature just above the water boiling point (usually 105 or 110 °C), applying vacuum, storing a sample in a dry environment (e.g., in desiccator), or a combination of the above, are routinely applied to remove molecular water. Smectites and interstratified minerals with smectitic surfaces, like illite-smectite, contain adsorbed water molecules even after extensive drying at temperatures above 100 °C (e.g., Mooney et al. 1952; Cuadros et al. 1994a; Środoń and McCarty 2008). This residual, tightly bound water (TBW) can persist up to temperatures overlapping with the beginning of dehydroxylation, contrary to the weakly bound water (WBW) that can be removed by drying at temperatures ≤ 110 °C (Cuadros et al. 1994a; Marumo et al. 1995; Cases et al. 1997; Środoń and McCarty 2008). The boundary between WBW and TBW is purely operational, depends on the actual drying conditions, and is not related to any particular transition in H_2O molecules position or bonding. Despite numerous studies on smectite dehydration, a systematic study on the quantification of TBW in smectites with various 2:1 layer structures and interlayer cations subjected to different drying protocols is missing. Such an exact quantification of TBW and understanding of the mechanism of TBW retention and removal is required when for e.g., analyzing oxygen, and the hydrogen stable isotope composition of 2:1 phyllosilicates (Marumo et al. 1995; Savin and Hsieh 1998; Bauer and Vennemann 2013), unraveling details of smectite dehydroxylation (Bray and Redfern 2000; Drits et al. 2012) and rehydroxylation (Derkowski et al. 2012a), determining ineffective versus effective porosity, and other petrophysical properties of hydrocarbon reservoir rocks (e.g., McCarty et al. 2015; Topór et al. 2016). Smectites are often considered as a landfill barrier in nuclear waste disposal sites, where heat is generated, therefore

59 understanding the nature and kinetics of smectite dehydration contributes to predicting long-term
60 changes of smectite sealing properties (Ferrage et al. 2007a; Kaufhold and Dohrmann 2010).

61 The hydration enthalpy of an interlayer cation is the main factor controlling the amount of
62 water adsorbed in a smectite interlayer at a given relative humidity at a temperature below 100 °C
63 (Bérend et al. 1995; Cases et al. 1997; Cuadros 1997; Chiou and Rutherford 1997; Ferrage et al.
64 2007a; Derkowski et al. 2012b), with layer charge density and layer charge location playing a
65 secondary role (Sato et al. 1992; Ferrage et al. 2007c; Środoń and McCarty 2008). There is no
66 agreement regarding the temperature at which TBW is completely removed and dehydroxylation
67 starts: while Emmerich et al. (1999) assigned the mass loss between 200 and 350 °C to the
68 dehydroxylation of weakly bonded OH groups, other researchers interpreted a low-rate mass loss
69 measured by thermogravimetry (TG) up to 500 °C as the removal of residual water (El-Barawy et
70 al. 1986; Bérend et al. 1995; Cases et al.1997). Using TG and magic-angle spinning nuclear
71 magnetic resonance (MAS-NMR), Kloprogge et al. (1992) suggested that a complete dehydration
72 of Na-exchanged beidellite occurs at around 400 °C. While the presence of TBW is not easily
73 identifiable, its quantification is even more difficult. The TBW content of 3.3 wt% in smectite
74 samples dried above 200 °C were reported by Cuadros et al. (1994a) who used Differential
75 Thermal Analysis (DTA). The content of residual water in the SWy-2 reference smectite was
76 reported to vary between 4.4 and 1.8% and between 3.0 and 1.7% of the final mass for divalent
77 and monovalent interlayer cations, respectively, as determined with Controlled Rate Thermal
78 Analysis (CRTA) under dynamic vacuum (Bérend et al. 1995; Cases et al. 1997). Using the same
79 method, Michot et al. (2005) found the TBW content in Na-saponite at 110 °C to vary between
80 0.5 and 0.6 water molecule per exchangeable cation (H_2O/EXCH; mol/mol). Środoń and
81 McCarty (2008) determined that the TBW content was between 0.7 and 2.2 wt% for a series of

Ca-exchanged smectites using TG experiments involving 24 hours of pre-drying at 200 °C under dry nitrogen purge. As inferred from these studies, the TBW contents determined with different methods are similar but a systematic comparison of TBW contents in various smectites is lacking.

Smectite dehydration is a multi-step reaction involving probably simultaneous first-order nucleation-growth and two-dimensional diffusion-controlled steps (Bray and Redfern 1999; Ferrage et al. 2007b). In addition, during the last stages of the TBW removal, dehydration and dehydroxylation reactions overlap, as was inferred from thermogravimetric (Cuadros et al. 1994a; Cases et al. 1997) and isotopic (Marumo et al. 1995) studies. Due to the overlap of the processes, each involving multi-step reaction mechanisms, finding the activation energy of TBW removal using model-fitting techniques is challenging (Poinsignion et al. 1982; Bray and Redfern 1999; Ferrage et al. 2007b). In contrast, the model-independent isoconversional methods have been successfully applied to smectites, thus they seem to offer a potentially more robust alternative for determining E_a (Prado and Vyazovkin 2011). The described overlap implies that TG experiments allow, at most, only to calculate the apparent apparent E_a, which is an average value of contributions by each of the simultaneous processes at a given degree of reaction (Vyazovkhin et al. 2011).

Only a few publications on the kinetics of smectite dehydration differentiate between different types of adsorbed water. For Ca-montmorillonites, using isothermal TG experiments, Bray and Redfern (1999) found that between 20 and 150 °C water is removed in two stages: the first one occurring below 90 °C was nucleation and growth controlled with E_a from 28.6 kJ/mol to 40.6 kJ/mol and the second took place above 90 °C (closely corresponding to TBW defined in this study) and was diffusion controlled with E_a equal to 47 ± 6 kJ/mol. The latter E_a range was approximately four times lower than the E_a of 185 kJ/mol reported for other Ca-montmorillonite

by Poinsignon et al. (1982) who used a non-isothermal TG run , which may partially explain the obtained differences. Ferrage et al. (2007b) described a multiple reaction mechanism of smectite dehydration involving the first dehydration stage with E_a of 84(2) kJ/mol and the second dehydration stage (approximately corresponding to TBW definition) with E_a of 127(5) kJ/mol. The E_a values of the second step of dehydration of Ca-exchanged samples reported in other studies (Girgis et al. 1986; Ferrage et al. 2007b; Prado and Vyazovkin 2011) lay in between the boundary values of Bray and Redfern (1999) and Poinsignon et al. (1982). Both the ranges of E_a reported for subsequent steps of smectite dehydration and the differences in E_a calculated using different methods closely correspond to those found for zeolites (cf. Hunger et al. 1999 to Dima and Rees 1987).

The aim of the present studyis to provide a systematic and reliable calculation of TBW amounts and to constrain the apparent E_a of TBW removal for selected representative smectite samples with different interlayer cations. The results reveal potential pitfalls in commonly applied drying protocols and attempts to determine optimal drying conditions for smectites and other smectite interstratified clays. The results obtained were compared against TBW contents in zeolites that served as apparently OH-free reference materials. It is worth emphasizing that the expression "tightly bound water" (TBW) is used in the present study to describe molecular water that remains in the sample after at least four hours of drying at a temperature of 110 °C or greater.

Materials and methods

Materials

This study was based on four natural dioctahedral montmorillonites and one synthetic saponite (Table 1), the same as used in Kuligiewicz et al. (2015). Two trans-vacant high-charge montmorillonites: SAz-2 and SCa-3, one cis-vacant low-charge beidellitic montmorillonite (SWy-2), and one ferruginous low-charge smectite (SWa-1, often considered as nontronite) were obtained from The Clay Minerals Society Source Clay Repository. The synthetic saponite (SAP) was a high-charge specimen of the trioctahedral series studied by Pelletier et al. (2003).

Two synthetic zeolites: 4A with chemical formula $Na[(AlO_2)_2(SiO_2)_2] \cdot nH_2O$ and 13X with chemical formula $Na_{86}[(AlO_2)_{86}(SiO_2)_{106}] \cdot nH_2O$ obtained from Fluka (CAS No 63231-69-6), and Avantor Performance Materials (former POCH, CAS No 1318-02-1), respectively, were additionally used as reference materials (Derkowski et al. 2007).

All dioctahedral smectite samples were purified by removing carbonates, organics, and Fe-(oxy-)hydroxides by a sequence of acetic acetate buffer, hydrogen peroxide, and buffered sodium dithionite treatments (Jackson 1969). The SWa-1 sample did not undergo dithionite treatment in order to avoid a potential alteration of the structure (Środoń et al. 2009). Purified samples were washed in deionized water. Subsequently, grain size fractions were separated by centrifugation. The XRD-based impurity-free grain size fractions were selected (Table 1) in order to ensure adequate purity of each smectite sample used in the experiments. Homoionic forms of each smectite were prepared by five washings with appropriate 0.5 M Mg^{2+}, Ca^{2+}, Na^{+}, or Cs^{+} chloride solutions of a reagent grade purity in at least 10-fold excess of a sample CEC, followed by dialysis in deionized water with a total contact time between water and the sample less than three days. Zeolites were gently crushed in an agate mortar and reacted with 0.5 M solutions of Na^{+}, and Ca^{2+} chlorides, followed by dialysis in deionized water.

148 **TG experiments for determination of tightly bound (residual) water content**

149 The thermal analyzer TA Discovery by TA Instruments with an absolute weighing error
150 of <1 μg, weight measurement resolution of <0.1 μg, and a thermal drift between 200 and 1000
151 °C of <4 μg was used. The initial sample mass of the air-dry smectites was 20 mg. The TG
152 analyzer was coupled with a quadrupole mass spectrometer ThermoStar by Pfeiffer Vacuum for
153 analysis of the evolved gases. The TG experiments were performed in a dry nitrogen (purity >
154 99.999%; supplied by Air Products) flow at 100 ml/min rate.

155 In order to calculate the TBW contents, two types of TG experiments were performed
156 (Fig.1): one involving a single isotherm heating and another involving a multiple isothermal
157 heating. The single isothermal heating experiments (SIH) involved one isothermal heating
158 segment at 110 °C, 200 °C, or 300 °C, for 4, 6, or 12 h followed by a ramp heating to 1000 °C
159 with a 5 °C/min rate. The SIH experiments are further labeled as xCyH-SIH where xC is the
160 isothermal heating temperature (in °C), and yH is the isothermal drying time (in hours).
161 Correspondingly, the end of the isothermal heating segment in a particular SIH experiment is
162 referred to as EI-xCyH-SIH (Fig. 1). The multiple isothermal heating experiments (MIH)
163 consisted of three consecutive isothermal heating segments at 110 °C, 200 °C, and 300 °C
164 separated by a ramp heating at a 5 °C/min rate and followed by a ramp heating to 1000 °C at 5
165 °C/min at the end of the experiment (Fig. 1). End points of these isothermal heating segments are
166 labeled EI-xC-MIH, where x is the isothermal heating temperature (in °C). The total time, from
167 the beginning of the experiment to the end of the first isothermal heating segment and between
168 the ends of two consecutive isothermal heating segments, i.e., between EI-110C-MIH and EI-
169 200C-MIH, and between EI-200C-MIH and EI-300C-MIH, was always 4 h (Fig. 1). The time of
170 heating of the TG furnace from room temperature to the temperature of the first isothermal

heating segment was less than 1 minute ("ballistic" heating mode) for both SIH and MIH experiments.

TBW contents were calculated using the following assumptions: a) dehydroxylation reaction of 2 OH → $H_2O\uparrow + O_r$, where O_r is the residual oxygen, was valid for all samples (Drits et al. 1995); b) samples at 995 °C were completely dehydrated and dehydroxylated; c) samples were monomineralic (negligible content of impurities) with exchangeable cations composition homoionic enough (cf. Steudel and Emmerich 2013) for reliable measurement of experimental mass loss (Δm_{exp}, Fig. 1) relevant to the theoretical smectite mass loss Δm_{DX} calculated from the chemical formulae (Table 1). All mass loss events, unless stated otherwise, were attributed to the loss of H_2O. TBW contents in wt% of dehydroxylated structure mass (TBW% in Fig. 1) were determined by subtracting theoretical mass loss of dehydroxylation Δm_{DX} from the mass loss measured in a TG experiment, Δm_{exp}. Experimental mass loss was normalized to a sample mass at the end point of the experiment ("EP" in Fig. 1). EP was usually set at 995 °C i.e., mass of dehydroxylated structure was used, as the most unambiguous value. Exceptions from the EP location at 995 °C are discussed later in the text. The calculation method applied was similar to those used in the other TG studies on smectite dehydration (Bérend et al. 1995; Cases et al. 1997; Cuadros et al. 1994a; Michot et al. 2005; Środoń and McCarty 2008).

The temperatures of virtual onset of dehydroxylation (TVD) were defined as the temperatures corresponding to the point on a TG curve at which the remaining mass loss to EP equals Δm_{DX} (Fig. 1).

Calculation of activation energy

193 The activation energy of dehydration was calculated for selected samples from two types
194 of TG experiments: with and without the isothermal heating segment prior to the ramp heating. In
195 the experiments without the isothermal heating segment, a ramp heating from room temperature
196 to 1000 °C was performed with five different heating rates, between 1 and 20 °C/min, using 25
197 mg of a sample. The experiments involving the isothermal heating segment were the 110C4H-
198 SIH experiments repeated five times applying different heating rates for the ramp heating
199 segment, between 2 and 20°C/min, using 20 mg portions of a sample. Na- and Ca-exchanged
200 SAz-2, SCa-3, and SWy-2 smectites were used in the experiments without the isothermal heating
201 segment, while the experiments involving the isothermal heating segment were performed for
202 Mg- and Na-SAz-2, Mg-, Ca-, Na-, and Cs-SCa-3 smectites as well as for Ca-13X zeolite.

203 Two model-independent isoconversional methods of E_a calculation were applied: the
204 Friedman method and the Kissinger-Akira-Sunose method (KAS method; Vyazovkin et al. 2011).
205 Both methods use the isoconversional principle to the general kinetic equation:

206 $$\frac{d\alpha}{dt} = Ae^{\frac{-E_a}{RT}} f(\alpha) \qquad \text{Eq. 1}$$

207 where α is the degree of reaction at time t, A is the pre-exponential factor, R is the gas constant, T
208 is temperature in K, and f(α) is a function of α that depends on the reaction mechanism. After
209 transformation, the Eq. 1 is presented:

210 $$\int_0^{\alpha} \frac{d\alpha}{f(\alpha)} = A\int_0^{t} \exp\left(\frac{-E_a}{RT}\right)dt \qquad \text{Eq. 2}$$

211 The left hand side of Eq. 2 is usually written as g(α). When a linear heating rate (ß) is used i.e.,
212 T= ßt, the integral with respect to time can be changed to the integral with respect to temperature
213 and Eq. 2 becomes:

214 $$g(\alpha) = \frac{A}{\beta}\int_0^T \exp\left(\frac{-E_a}{RT}\right)dT \qquad \text{Eq. 3}$$

215 The isoconversional principle states that at a given degree of reaction, f(α) or g(α) and A both
216 have constant values, regardless of the temperature (Vyazovkin et al. 2011). In the case of non-
217 isothermal TG runs, this means that E_a can be calculated from experiments performed with at
218 least three different heating rates. The Friedman method is based directly on the logarithmic form
219 of Eq.1 and E_a is calculated from the relationship of ln(dα /dt) vs. 1/T. The KAS method is based
220 on Eq. 3, which, however, does not have an analytical solution. Numerical approximation of the
221 integral from Eq. 3 applied in the KAS method leads to the Kissinger-Akira-Sunose equation:

222 $$\ln\left(\frac{\beta}{T^2}\right) = C - \frac{E_a}{RT} \qquad \text{Eq. 4}$$

223 where C is the constant. E_a is calculated from the $\ln(ß/T^2)$ vs. 1/T plot (Vyazovkin et al. 2011).

224 The Friedman method requires numerical differentiation when applied to TG data, which
225 may be a source of error. No numerical differentiation of TG data is required in the KAS method
226 but the numerical approximation of integral from Eq. 3 implemented in this method is also a
227 source of error, but of a different origin than in the Friedman method. For both methods α was
228 calculated from:

229 $$\alpha = \frac{m_{start} - m}{m_{start} - m_{end}} \qquad \text{Eq. 5}$$

where – m_{start} is mass at the beginning of the reaction, m is the instantaneous mass, m_{end} is the mass at the end of the reaction.

WBW content in the portions used in experiments might have varied within narrow limits, because no conditioning of air-dry samples was applied before the start of the TG runs. In order to compensate for this scatter in the initial WBW content in the experiments without the isothermal heating segment, m_{start} was set as the mass corresponding to the point of the greatest adsorbed water content common for all five separate runs with different heating rates. Therefore m_{start} was not connected with any particular temperature. Such a procedure was applied to ensure that the calculations were performed on data referring to exactly the same fraction of water in each non-isothermal run. TVD was used as m_{end}, because these experiments aimed mostly at the calculation of E_a for WBW removal. For the experiments involving isothermal heating segments prior to the ramp heating, the differences in Δm_{exp} among TG runs for the same sample were less than 6.5% of the average Δm_{exp} value. As was discussed by Bray and Redfern (1999), minor variability in total mass loss among TG runs, which lead to the scatter of TBW content in the present study, does not impede the reliable calculation of E_a. Therefore, the masses at the end of isothermal heating segments were consequently used as m_{start}. The dehydration of TBW was poorly separated from dehydroxylation, therefore, the mass at 995 °C was used as m_{end}. The degree of reaction (α), defined in this way, clearly did not correspond to a single process, but comprised both TBW removal and dehydroxylation.

Sample purity

Although the samples underwent extensive purification with chemical and physical methods, and the purity was confirmed by the means X-ray diffraction (data not shown), and infrared spectroscopy (Kuligiewicz et al. 2015), minor insoluble amorphous or poorly crystalline impurities may persist. Some impurities, i.e., organic matter and poorly crystalline carbonates (formed from atmospheric CO_2 dissolved in a solution during cation exchange), can provide to observable mass loss even if present at low contents. These two most probable compounds evolve CO_2 upon heating. Therefore, in selected experiments, the sample purity was monitored with mass spectrometry (MS) of evolved gases. For the samples SWa-1 and SWy-2 an increase of the m/z 44 amu signal associated with separate, high temperature mass loss events were observed at temperatures about 800 °C that were not associated with the increase of m/z 18 amu signal coming from the evolved H_2O (Fig. 2).These high-temperature mass loss events were ascribed to the decomposition of traces of organic matter or carbonates. In the case of SWa-1, the high-temperature mass loss event was well-separated from the major DTG peak of dehydroxylation, because the latter reaction occurs at temperatures >100 °C lower than in other *trans*-vacant smectites due to high iron content (Frost et al. 2000; Ding and Frost 2002; Środoń and McCarty 2008) (Fig. 2). This enabled the compensation of additional mass loss by selecting EP at the minimum of DTG curve in the 500 - 600 °C range (Fig. 2). In the case of SWy-2, mass loss correction was calculated based on mass loss above 740 °C, associated with a release of CO_2, and equal to 0.3 wt% (Fig. 2).

TBW content and E_a calculations precision

All the analyzed samples show a major mass loss between 300 and 1000 °C, related to dehydroxylation (Fig. 3). The precision and accuracy of measuring mass loss during that thermal event contributes most to the precision of TBW content calculation. The credibility of the

computed TBW contents (in wt%) was tested by triplicating the 110C4H-SIH experiments with the SAz-2 sample in each cationic form studied. The average standard deviation (2σ) of TBW content from the total of 12 analyses was equal to 0.31 wt%. The observed variability could result from a combined sample heterogeneity or packing effects (cf. Bray and Redfern 1999) and the TG instrument precision. The precision obtained, however, refers to the samples with a well-defined EP localized at a TG plateau following the main dehydroxylation DTG peak. In case of the SWa-1 sample, the EP does not meet these requirements, therefore, the TBW error is supposedly greater.

The average E_a calculation error was estimated at 7 kJ/mol on the basis of uncertainty of regression equations for all points with $r^2>0.9900$. However, if E_a seemed stable over a certain α interval, as determined by the visual inspection of E_a vs. α plots, then standard deviation (1σ) of E_a over that interval was assumed to be a more reliable estimate of measurement error and values based on 1σ, if available, are given.

Results

Mass evolution in the isothermal segments

All samples showed similar trends in the evolution of mass loss over time in the isothermal segments of SIH experiments. Mass loss was the fastest at the beginning of the isothermal drying, became slower and the TG curve eventually reached a stable mass interval for Ca-, Na-, and Cs-exchanged forms (Fig. 4). For the Ca-exchanged samples, the TG plateau, i.e., the stable TBW content, was reached after less than 1 h of isothermal drying while in the case of Cs- and Na-forms, this was achieved in less than 30 min. In the Ca-, Na-, and Cs-exchanged SAz-

296 2, TBW content remained the same after 4, 6, and 12 h of drying (Table 2). In the case of Mg-
297 exchanged smectites, the isothermal heating at 110 °C for 4 h did not lead to a stable TBW
298 content, which, in contrast, seemed to be the case in 200C4H-SIH experiments. For 300C4H-SIH
299 experiments, the Mg-SAz-2 showed a less-defined plateau than after heating at lower
300 temperatures (Fig. 4). In that sample, stable mass was not reached even after 12 h of drying at
301 110 °C, 200 °C, or 300 °C (Fig. 4).

302 The lack of stable mass intervals for Mg-exchanged smectites could also be visible in the
303 MIH experiments (Fig. 4). The Mg-exchanged samples showed a rapid mass loss during the first
304 isothermal heating segment at 110 °C, which continued during the following isothermal heating
305 segments, although at a lower rate. Those mass loss intervals were separated by more rapid mass
306 loss events during the ramp heating segments. In contrast, Cs-exchanged samples quickly
307 attained stable mass intervals each time after the temperature reached a subsequent isothermal
308 segment in MIH experiment, similar to the trends observed in the SIH experiments (Fig. 4). Na-
309 and Cs-exchanged samples behaved similarly, while Ca-exchanged smectites displayed behavior
310 intermediate between Mg-, and Cs-exchanged ones, with pronounced stable mass intervals at
311 each isothermal heating segment, preceded by approximately 1 hour long mass loss intervals
312 (data not shown).

313 Noticeably, the SWa-1 sample, in any cation form, did not reach stable mass during the
314 isothermal heating at 300 °C neither in SIH, nor in MIH experiments (data not shown).

315 **Mass evolution in the ramp heating segments**

316 In all experiments, DTG patterns of the final ramp-heating segments were dominated by a
317 dehydroxylation peak at 400-700 °C for dioctahedral, and 700-900 °C for trioctahedral samples

(Fig. 3). The temperature range and shape of this peak corresponded to those known from the literature for a given smectite and were slightly affected by the interlayer cation type. The temperature of the maximum of dehydroxylation rate (TDX) followed the order known for these samples from the literature, SAP > SWy-2 > SAz-2 ≥ SCa-3 > SWa-1 (e.g., Derkowski et al. 2012b).

Ca-, Na-, and Cs-exchanged SAP, SAz-2, SCa-3, and SWy-2 samples displayed shoulders on the low-temperature side of the main dehydroxylation DTG peak, attributed to the loss of TBW, which became less pronounced with increasing isothermal heating temperature (Fig. 3). The shoulder could not be observed for SWa-1 sample due to a too low a temperature of dehydroxylation reaction (Fig 3). In the 110C4H-SIH experiments all Mg-smectites displayed two dehydration DTG peaks preceding the main dehydroxylation event: first and usually the most pronounced at approximately 190 °C, and the second between 300 °C and 400 °C. The second dehydration DTG peak was still visible in the 200C4H-SIH experiments and remained detectable as a low-temperature shoulder of the dehydroxylation DTG peak in the 300C4H-SIH experiments. The second DTG peak was not observed for Mg-SWa-1, probably because of an overlap with dehydroxylation.

In the case of SAP, DTG features corresponding to dehydration and dehydroxylation were well separated, and the overlap between them was largely reduced, especially in the Cs-exchanged form (Fig. 3). Interestingly, in Mg-SAP mass loss continued up to the beginning of the dehydroxylation DTG peak (> 650 °C), while in the Cs-SAP mass loss was negligible before the onset of dehydroxylation. Mg-SAz-2 showed a second DTG peak corresponding to dehydroxylation, at ~900 °C, which was also observed in the Mg-SCa-3 and – to a much lower

extent – in Mg-SWy-2. The relative area of that DTG peak seemed to increase with the temperature of the isothermal segment (Fig. 3).

Tightly bound water (TBW) content

As expected, in xC4H-SIH experiments, the highest amount of TBW for a particular sample was observed after isothermal drying at 110 °C, followed by the TBW contents at EI-200C4H-SIH and EI-300C4H-SIH. The variability of TBW content at EI-xC4H-SIH experiments matches the TBW content at the corresponding points in MIH experiments, differing randomly by an absolute average of 0.19 wt%, thus below the TBW content determination error, which provides independent validation of the TG results (Table 3). After isothermal drying at 110 °C or 200 °C, both in SIH and MIH experiments, TBW contents generally depend on the exchangeable cation, in the following order Mg > Ca > Na ≥ Cs (Table 3). The MIH of SWa-1 is an exception not matching that trend, likely due to the unstable EP. In addition, all SWa-1 samples heated isothermally at 300 °C, in both SIM and MIH experiments, showed negative TBW contents, which was not observed after drying at lower temperatures (Table 3). The negative TBW clearly imply that during isothermal drying at 300 °C of SWa-1 partial dehydroxylation occurs, which is in agreement with other TG studies of this sample (Ding and Frost 2000; Środoń and McCarty 2008). Therefore, the data of SWa-1 heated at 300 °C were not used for subsequent calculations.

After drying at 300 °C, all samples had a small (usually ≤0.8 wt%) TBW content whose dependence on the interlayer cation type became less clear. The difference among TBW contents fell within the measurement precision limit (Table 3) for this heating temperature, with the exception of SAP samples, whose TBW content in the Mg-exchanged form was still much greater than in other cationic forms, both in the SIH, and MIH experiments (Table 3).

When comparing TBW content between different samples, the H_2O/EXCH (mol/mol) ratio that is the total residual H_2O content normalized to the quantity of interlayer cations known from the chemical formula, was found to be more informative than the TBW contents in wt%. This is because H_2O/EXCH takes into account the absolute number of cations in the unit cell, which is controlled by the 2:1 layer charge and cation valence. The pattern of H_2O/EXCH cation-dependency is common qualitatively and quantitatively for all studied samples heated under given conditions (Fig. 5). Monovalent cation-exchanged smectites require 300 °C for complete dehydration, although even 200 °C seems sufficient for some Cs-exchanged smectites to lose TBW completely. TBW in Ca-exchanged smectites is always higher than in their monovalent analogs and drying at 300 °C does not remove TBW completely. Mg-exchanged smectites retain more H_2O molecules per interlayer cation than other cations for the same drying temperature, however, Mg-exchanged high-charge montmorillonites seem to retain less H_2O at EI-300C4H-SIH and EI-300C-MIH than Mg-SAP and Mg-SWy-2 samples (Fig. 5). A comparison between the SIH and MIH experiments revealed good reproducibility of TBW contents for corresponding drying conditions (Table 3 and Fig. 5).

Temperature of virtual onset of dehydroxylation (TVD)

The computed TVDs showed no correlation with interlayer cation type, neither with the isothermal heating temperature nor time. Instead, the TVD varied within quite a narrow range for a given smectite, showing a standard deviation of 17-31 °C range (Fig. 3 and Table 4). The average TVDs seem to correlate with TDX: the highest (TVD 559+/-31 °C) for the trioctahedral SAP, then the cis-vacant SWy-2 (445+/-21 °C), followed by the apparently trans-vacant Mg-rich

montmorillonites (TVD 388-407 °C). SWa-1 had the lowest TVD, which was calculated only for the experiments that did not involve isothermal heating at 300 °C due to sample dehydroxylation. For SWa-1, divalent cation forms showed TVD a little above 300 °C, while Cs and Na forms had TVD below 300 °C (Table 4). In general, the Cs-exchanged samples showed more variable TVD than other cationic forms, as well as SAP did in respect to other samples. In such cases where TDX is high and TBW content is low, the TVD point was positioned on a DTG plateau occurring before the beginning of the dehydroxylation peak, therefore, small changes in TBW content could produce relatively large differences in TVD. Dioctahedral smectites had the TVD point positioned at a shoulder of the major DTG peak representing dehydroxylation (Fig. 3).

Tightly bound water in zeolites

Two synthetic zeolites were examined using xC4H-SIH experiments. The TBW content in zeolites was calculated as a difference between the mass at the end of isothermal heating segment and EP at 995 °C, normalized to the mass at EP. A minute mass loss above 800 °C was observed for zeolite 13X (Fig. 6), however, no mass loss correction was applied. After an isothermal heating, zeolite 4A had on average a greater TBW content than zeolite 13X. Similarly, Ca-saturated zeolites showed higher TBW contents than their Na-saturated analogues. After drying at 300 °C, 1.2, and 1.9 wt% of TBW were still present in the Ca-exchanged 13X, and 4A, respectively (Table 5). However, H_2O/EXCH ratios for the studied zeolites were very similar to those of smectites (Fig. 5). Because in the 110C4H-SIH experiments on zeolites the mass loss curve did not reach plateau (data not shown), TBW contents calculated for these runs may be overestimated.

Activation energy

406 E_a values are reported for both the KAS and Friedman method calculations only for the
407 results of the Ln(dα/dt) vs. 1/T or Ln(ß/T2) vs. 1/T correlations for which the R^2 coefficients
408 were greater than 0.9900 (Fig. 7). The average differences between E_a calculated with the
409 Friedman and the KAS methods varied between 2 and 7 kJ/mol for experiments with the
410 isothermal heating segment. The difference was highest for low and high ends of a reaction
411 extent, which is a known methodological effect (Vyazovkin et al. 2011). Systematic differences
412 between E_a from the two methods were smaller than the calculated E_a precision, therefore, only
413 one set of the results is sufficient for further discussion, and the E_a results hereafter are reported
414 from the Friedman method only, because it is potentially more accurate. Due to the fact that the
415 degree of reaction (α) was calculated on the basis of mass loss, α can be directly recalculated to
416 the TBW or WBW contents, or to H_2O/EXCH (e.g., Fig. 8). In the case of experiments without
417 the isothermal heating segment, the KAS method produced erratic R^2 values and inconsistent
418 trends of E_a of WBW dehydration, which, however, tended to converge with E_a values from the
419 Friedman method with an increasing degree of reaction (α). E_a values obtained with the KAS
420 method were disregarded in this case.

421 In the kinetic experiments without the isothermal segment, E_a values of WBW removal
422 for SAz-2, SCa-3, and SWy-2 samples were similar to each other in both the Ca-, and Na-
423 exchanged sample sets (Fig. 8). Ca-exchanged samples showed a small and consistent increase of
424 E_a, from 45-48 kJ/mol at H_2O/EXCH=10 to E_a of 3-4 kJ/mol greater at H_2O/EXCH=5. At lower
425 H_2O/EXCH ratios, E_a increased and reached 61-64 kJ/mol in Ca-SWy-2 and Ca-SCa-3, and 76
426 kJ/mol in Ca-SAz-2 at H_2O/EXCH~3. Na-exchanged SCa-3 and SWy-2 reached stable E_a values
427 near 48 kJ/mol, while Na-SAz-2 showed a slightly different behavior. Its E_a of WBW removal

428 increased from the value corresponding to the E_a plateau in two other smectites at H_2O/EXCH =
429 3.0-3.5 to E_a of 56+/-2 kJ/mol at H_2O/EXCH of 1-2 (Fig. 8).

430 The pattern of E_a evolution with α determined in the experiments involving the isothermal
431 heating segment differed significantly between the cationic forms of the tested smectites (Fig. 9).
432 The Cs- and Na-exchanged SAz-2, and SCa-3 samples show a broad plateau of E_a in the range of
433 20-70% degree of dehydroxylation (DX). The E_a calculation for TBW removal did not meet the
434 correlation fit requirement of $R^2 > 0.9900$, therefore, it was not reported, except for the Na-SCa-
435 3, which returned statistically significant values of 150-180 kJ/mol when approaching TVD. The
436 plateau of E_a of dehydroxylation occurred in Cs- and Na-exchanged SCa-3 at almost identical
437 values of 230-237 kJ/mol, making the value reliable as true E_a of dehydroxylation. In the case of
438 Na-SAz-2, the plateau is less defined and remains at 233+/-5 kJ/mol (Fig. 9), while its Cs-
439 exchanged analog shows a plateau at 249 +/-2 kJ/mol (data not shown).

440 For Ca-SCa-3, E_a first steadily increased from 102 kJ/mol at TBW≈1wt% and reached the
441 point corresponding to TVD with E_a=189 kJ/mol (Fig. 9). At an inflection point with E_a=214
442 kJ/mol, the slope flattens and E_a values reach 253 kJ/mol at the end of dehydroxylation. In the
443 Ca-SAz-2 sample, the E_a trend line flattens, reaching a broad maximum of 216+/-5 kJ at 20-75%
444 DX (data not shown).

445 Mg-exchanged SCa-3 and SAz-2 samples, presented a steady increase of E_a between 2-3
446 wt% TBW, and ~50% DX, from 88 kJ/mol to 224 kJ/mol, and from 72 kJ/mol to 166 kJ/mol for
447 Mg-SCa-3, and Mg-SAz-2, respectively, with variably decelerating rates of the E_a increase. In
448 both cases a broad hump of E_a curve at advanced dehydroxylation could be noticed. In both
449 samples, no plateau for E_a was reached and the average E_a for the hump corresponding to

dehydroxylation was lower than that determined in the corresponding smectites exchanged with monovalent cations: by ~ 25 kJ/mol in the SCa-3 and even ~ 80 kJ/mol for the SAz-2 sample (Fig. 9). The TVD point for Mg-SCa-3 was found in the middle of a steady slope and corresponding to E_a of 161 kJ/mol while Mg-SAz-2 had the TVD point at the beginning of a slower E_a increase interval, with E_a equal to 140 kJ/mol.

The calculation of TBW removal for the Ca-exchanged zeolite 13X determined after isothermal drying at 110 °C, using the Friedman method returned values increasing from 85 kJ/mol at H_2O/EXCH = 0.9 to 164 kJ/mol at H_2O/EXCH = 0.15, very similar to E_a of TBW removal for the Ca-SCa-3 sample in the same H_2O/EXCH range (Fig. 10). The trend for the Ca-13X zeolite is more concave, with a slower increase of E_a values at higher H_2O contents than in the smectite sample.

Discussion

Factors affecting the residual adsorbed water content

The TBW contents reported in the present work for Ca-exchanged samples dried at 200 °C agree well with the data presented in Środoń and McCarty (2008) for the same smectites, with differences between 0.1% for SWa-1 and 0.7% for SWy-2. The adsorbed water contents in Na-exchanged saponite heated at 110 °C under dry (<5 ppm H_2O) nitrogen flow (H_2O/EXCH equal to 0.5, this study) is practically the same as in saponite with the same layer charge outgassed to a residual pressure of 2 Pa at 25 °C and 110 °C (H_2O/EXCH equal to 0.6 and 0.5 respectively; Table 1 in Michot et al. 2005). This similarity implies that reducing the partial pressure of water vapor over a sample is the key factor to reducing the adsorbed water content, regardless of the

472 actual method used to reduce the H_2O partial pressure. TBW contents reported in Table 3 for the
473 200C4H-SIH experiments are considerably smaller than those inferred from DTA and TG
474 experiments by Cuadros et al. (1994a) (cf. their Table 1). Because the experiments performed by
475 Cuadros et al. (1994a) did not involve the isothermal heating segment, and the samples used had
476 mostly Mg^{2+} as the interlayer cation (Cuadros 1994b; Dudek et al. 2006), the difference observed
477 between the present results and those from Cuadros et al. (1994a) may come from the kinetic
478 effect related to Mg hydration enthalpy, as discussed below.

479 The temperature of drying was the main factor controlling TBW content in the
480 investigated samples (Table 3), which is consistent with previous works on smectite dehydration
481 (Rinnert et al. 2005; Środoń and McCarty 2008). Interlayer cation hydration enthalpy was found
482 to be the main factor determining differences in the TBW content between samples heated
483 isothermally at the same temperature (Table 3 and Fig. 5). Correlation between the interlayer
484 cation type and the adsorbed water content reported in numerous studies (Cases et al. 1992;
485 Bérend et al. 1995; Cases et al. 1997) remains valid also for samples heated at and above 110 °C
486 (Table 3). Indeed, the TBW content was found to correlate quantitatively with the exchangeable
487 cation hydration enthalpy (Fig. 11).

488 With the exception of the Mg-exchanged specimens, the mass loss curves of all samples
489 in both SIH and MIH experiments reach a stable mass plateau after at most 1 hour of isothermal
490 drying, which implies that extending the time of drying does not decrease the TBW content
491 below the value controlled exclusively by the temperature, the interlayer cation hydration
492 properties, and the activity of water vapor in the sample environment, which is assumed to be
493 close to zero in the case of the present work. Such a conclusion is supported by a close agreement
494 between the TBW contents from the 300CMIH and 300C4H-SIH experiments, despite the fact

that at EI-300C-MIH the samples were subjected to temperatures greater or equal to 110 °C for more than 12 h in respect to 4 h at EI-300C4H-SIH (Table 3). No systematic relationship between the 2:1 layer structure and the TBW content were discerned for Ca-, Na-, and Cs-exchanged samples even for the TBW content, which are not normalized to the amount of interlayer cations, i.e., to layer charge, which remains in agreement with findings of Środoń and McCarty (2008).

Mg-exchanged smectites have distinctly different properties with respect to other cationic forms of the studied samples. They do not reach stable mass even after prolonged drying i.e., the TBW content decreases with time (Table 3), which is probably associated with the ability to retain more water molecules at high temperatures due to the high hydration enthalpy of Mg^{2+} (Fig. 5 and 11). The effect of high hydration enthalpy on mass loss signature of Mg-exchanged samples is the best visible for SAP, that has well separated dehydration and dehydroxylation DTG peaks, due to its trioctahedral structure (Fig. 3). Cs-exchanged SAP presents the lowest TBW contents among all cationic forms of this sample due to the low hydration enthalpy of Cs^{+} (Fig. 11) and its large size that makes interlayer space larger than in other cationic forms, facilitating dehydration (cf. Derkowski et al. 2012b). The mass loss rate for this sample drops to zero in a short interval between the main dehydration and dehydroxylation events (Fig. 3), in contrast to Mg-SAP, which still displayed measurable mass loss at this interval.

Mg-exchanged samples are the only ones for which the charge location, hence 2:1 layer structure, played an important role during dehydration, due to the small radius of Mg^{2+}. High-charge dioctahedral montmorillonites, i.e., SCa-3 and SAz-2, had similar, very low H_2O/EXCH ratios in all cationic forms after drying at 300 °C, while other smectites tended to have higher H_2O/EXCH ratios in their Mg-exchanged forms (Fig. 5). SCa-3 and SAz-2 both have high octahedral charge which may cause the migration of small cations into the 2:1 layer structure

(Hoffman-Klemen effect), which was suggested to occur not only for Li^{+}, but also for Mg^{2+} (Calvet and Prost 1971; Kawano and Tomita 1991) and other small divalent cations (Emmerich et al. 2001). Apparently at 300 °C a number of water molecules in Mg^{2+} hydration sphere is reduced enough to allow some of the interlayer Mg^{2+} to move through the ditrigonal cavity and to bind directly with the octahedral sheet's oxygen atoms, which results in the release of the final fraction of H_2O, thus the decrease of H_2O/EXCH ratio (Fig. 5). The resulting dehydrated structure is then more heterogeneous than the starting one, because it has one population of the former interlayer Mg^{2+} fixed within 2:1 layer and the other population remaining in the interlayer space (Calvet and Prost 1971).

Differentiating between WBW and TBW in kinetic experiments

In the present study TBW is arbitrarily defined as H_2O remaining in the sample after heating for at least 4 hours at temperatures ≥110 °C. Discrimination between WBW and TBW is thus straightforward in all experiments that involve the isothermal heating segment. However, if no isothermal heating is applied, as is the case for a part of the kinetic experiments (Fig. 8), the unambiguous distinction is not readily available.

The kinetic experiments are able to differentiate between the bulk interlayer water and H_2O from the hydration spheres of interlayer cations, and are able to detect the reconfiguration of water molecules in the hydration sphere, which causes the decrease of interlayer space due to advancing dehydration (cf. Bray and Redfern 1999; Ferrage et al. 2007b for Ca-exchanged smectites). However, in the kinetic experiments without the isothermal heating segment aiming at WBW these phenomena seem to not occur at water contents predicted for the first hydration sphere (Fig. 8). TBW contents in Na- and Ca-exchanges smectites at EI-110C4H-SIH are

approximately H_2O/EXCH=1 and H_2O/EXCH=0.5, respectively (Fig. 5), therefore, they correspond to only a fraction of H_2O in the first hydration shell of these cations, which is 8 and 6 H_2O molecules for Ca^{2+} and Na^{+} respectively (cf. Michot et al. 2005; Rinnert et al. 2005; Ferrage et al. 2007a,b; Ferrage et al. 2010). In TBW, all water molecules coordinate interlayer cations directly (Rinnert et al. 2005; Ferrage et al. 2007a,b). WBW, in turn, comprises different types of H_2O: physisorbed water molecules with surface of minerals, H_2O molecules in the interlayer not directly coordinated to the interlayer cations ("bulk" interlayer water), and a portion of water molecules from the first hydration spheres of interlayer cations. Therefore, comparing the E_a for WBW and TBW with those in literature of smectite dehydration bears an intrinsic mismatch coming from different conditions and methods used in previous studies.

E_a of smectite dehydration

E_a of dehydration calculated for Ca-exchanged smectites with H_2O/EXCH>5 and for Na-exchanged smectites from the experiments without the isothermal heating are in the 45-58 kJ/mol range, which is in between the values reported by Poinsignion et al. (1982) that fall in the clusters of 33-37 and 73-81 kJ/mol for divalent and monovalent cations, respectively (Fig. 8 and Table 6). The values bracketed by the latter range were also reported by Zabat and Van Damme (2000), Ferrage et al. (2007b), and Prado and Vyazovkin (2011) for the fraction of water approximately corresponding to WBW in the present study. E_a of dehydration increases to 62-72 kJ/mol for Ca-exchanged smectites at H_2O/EXCH<4.5 that is close to the ratio at which H_2O in the Ca^{2+} hydration sphere undergoes reconfiguration followed by the increase of dehydration E_a (Rinnert et al. 2005; Michot et al. 2005; Ferrage et al. 2007a,b). While the change in E_a of the Ca-exchanged samples at H_2O/EXCH ~ 4.5 suggests the presence of at least two reaction mechanisms, stable E_a for the Na-exchanged samples implies a single reaction mechanism across

563 the entire studied range of WBW removal. An insignificant increase of E_a for the Na-SAz-2
564 sample closely resembles the changes in E_a of the Ca-exchanged specimen if the difference in the
565 cations' valence is accounted for, which may be caused by an incomplete ionic exchange of the
566 Ca-form used in the exchange procedure.

567 In the experiments with isothermal heating segment, the Mg- and Ca-exchanged samples
568 show a continuous increase of E_a of dehydration from the H_2O/EXCH values of 2 and 1,
569 respectively, to TVD (cf. Fig. 9). The observed increase is between 76-161 kJ/mol and 102-189
570 kJ/mol for Mg- and Ca-exchanged samples, respectively, in accordance with the results of
571 Poinsignion et al. (1982; Table 6). The range of E_a values for TBW removal in Ca-SCa-3 sample
572 obtained in this study (102-189 kJ/mol) encloses the value reported for 1 to 0 water layer
573 transition by Ferrage et al. (2007b) for the Ca-SWy-1 sample which was 127(5) kJ/mol (Table 6).
574 Unfortunately, no reliable calculation of Ea of TBW removal, i.e. for H_2O/EXCH ratio between 0
575 and 0.5, could be made for the samples exchanged with monovalent cations. The ranges of the
576 adsorbed water content corresponding to the calculation of E_a of dehydration did not overlap
577 between the kinetic experiments with and without the isothermal heating segment (cf. Fig. 8 and
578 9). Nevertheless, an extrapolation of the trends visible for Na-SCa-3 (Fig. 9) to lower
579 H_2O/EXCH, suggests a continuous transition similar to that in the divalent cations-saturated
580 smectite. The continuous changes of E_a imply a gradual transition between different reaction
581 mechanisms (Criado et al 2008), in agreement with the postulated overlap of dehydration and
582 dehydroxylation.

583 Changes in E_a along with the progress of dehydration support the interpretation that
584 temperature is the primal control of the TBW content. For the initial stages of dehydration, E_a
585 remains constant or increases insignificantly along with a decreasing number of adsorbed water

586 molecules. This fraction of water molecules, which corresponds to the majority of WBW, can be
587 removed kinetically, by extending the time of drying (Fig. 8). In contrast, E_a of TBW dehydration
588 increases along with the reaction progress (Fig. 9), therefore, the removal of subsequent TBW
589 portions requires increase of the temperature. The increase continues even after theoretical
590 removal of all water molecules, i.e., beyond the TVD point towards advanced dehydroxylation
591 (Fig. 9, Ca- and Mg-exchanged smectites).

592 TBW represents the H_2O molecules strongly bound by electrostatic interactions in the first
593 hydration spheres of interlayer cations. Theoretical studies using Density Functional Theory
594 (DFT), showed that the difference in the total bonding energies between two hydration states
595 decrease with consecutive addition of water molecules to the cluster (cf. Table 2 and 3 in Pavlov
596 et al. 1998), e.g., the difference in total bonding energies between Mg^{2+} and $[Mg(H_2O)]^{2+}$ is 85.5
597 kJ/mol, between $[Mg(H_2O)]^{2+}$ and $[Mg(H_2O)_2]^{2+}$ is 70.9 kJ/mol, whereas between $[Mg(H_2O)_2]^{2+}$
598 and $[Mg(H_2O)_3]^{2+}$ is 55.1 kJ/mol. Corresponding values for Ca^{2+} are 56.9, 47.5, and 42.0 kJ/mol,
599 respectively (Pavlov et al. 1998). A similar trend was observed for Na^{+}-H_2O clusters modeled
600 with molecular mechanics (Merchant and Asthagiri 2006). The results of DFT and molecular
601 mechanics studies are in agreement with the increase of E_a values along with the TBW decrease
602 found in the present study. Removing each H_2O molecule reorganizes the bonding among the
603 remaining molecules and increases the energy required to remove each subsequent H_2O molecule
604 directly bonded to the interlayer cation (Fig. 9).

605 **Mutual interdependence of dehydroxylation and dehydration.**

606 TVD is a measure introduced in order to facilitate the understanding of the phenomena
607 occurring at a transition between dehydration and dehydroxylation. If dehydration and

608 dehydroxylation were completely separated, TVD would be a reference point corresponding to a
609 completely dry state, i.e., the absence of adsorbed water molecules with preservation of all
610 initially present structural OH groups. This ideal state of a sample is the goal of drying prior to
611 CEC, porosity, or stable isotope ratios measurements of smectite-reach samples (Środoń and
612 McCarty 2008; Savin and Hsieh 1998). Obtained results indicate, however, that this state is in
613 most cases hardly possible to achieve. TVD is highly positively correlated with TDX for all
614 studied samples (Table 4). TVD is, therefore, controlled by TDX and the temperature range over
615 which dehydroxylation occurs (i.e., a breadth of DTG dehydroxylation peak), with no systematic
616 influence of the interlayer cation type nor the temperature of isothermal heating segment, which
617 remains in agreement with the proposed kinetic model. If dehydration and dehydroxylation were
618 separate processes, TDX would not influence TVD. Furthermore, correlation between TVD and
619 interlayer cation type would then be expected, because the interlayer cation's hydration enthalpy
620 determines the amount of TBW present in a sample after drying.

621 The TVD value is a result of an interplay between dehydration and dehydroxylation. In
622 the case of dioctahedral smectites saturated with interlayer cations of a high hydration enthalpy,
623 this implies that TVD does not correspond to the ideally dry state for most of the samples. Only
624 in the case of Cs-SAP, TVD can be interpreted as the temperature when all molecular water is
625 truly removed, due to the combined effects of high TDX and small TBW content remaining after
626 drying, caused by a low hydration enthalpy of Cs (cf. Fig. 3 and 6). For all the remaining
627 samples, mass loss due to dehydroxylation below TVD is equal to mass loss due to dehydration
628 above TVD. Above TVD, the sum of mass loss due to dehydroxylation and dehydration of
629 remaining adsorbed water molecules is equal to the theoretical mass loss due to dehydroxylation
630 of all OH groups initially present in a sample. In this interpretation, a final loss of the last water

631 molecules originally present in the interlayers occurs at the beginning of dehydroxylation, when
632 interlayer space re-expands (cf. Drits et al. 2012). Dehydroxylation must, therefore, start at
633 temperatures lower than TVD. A loss of weakly attached OH groups, most likely those from
634 smectite's edges and outer surfaces, was suggested to occur at temperatures as low as 250-350 °C
635 for cis-vacant montmorillonite (Emmerich et al. 1999), which is below the TVD temperatures
636 calculated in this study (350-400 °C for trans-vacant montmorillonites; Table 4). TVD in the 350-
637 400 °C range corresponds to the beginning of dehydroxylation in trans-vacant smectites observed
638 in DSC curves reported by Wolters and Emmerich (2007). The gradual increase of E_a from
639 dehydration to dehydroxylation supports the interpretation of lower-than TVD temperature of an
640 onset of dehydroxylation described above.

641 Smectites exchanged with monovalent cations present a uniform plateau of E_a of
642 dehydroxylation over broad ranges of DX, with an average E_a equal to or higher than in their Ca-
643 exchanged analogs (Fig. 9, Table 6). Mg-exchanged smectites do not reach a plateau, with
644 maximum E_a always lower than in their analogs with different interlayer cations. The variability
645 of average E_a of dehydroxylation among different cation forms of SCa-3 and SAz-2 samples is
646 very similar to that reported by Bray and Redfern (2000) for Wyoming smectite. Quantitatively,
647 the E_a values calculated by those authors are also close to the values calculated for corresponding
648 cation forms of SCa-3 and SAz-2 despite using isothermal experiments, and different kinetic
649 models. The formation of trioctahedral domains caused by Mg-fixation was confirmed by the
650 increase of the DTG peak at temperatures ~900 °C for samples dried at 300 °C in respect to the
651 samples dried at lower temperatures. The high-temperature DTG peak was also increased for the
652 samples heated isothermally for a longer time(Fig. 3). Such a high-temperature DTG peak is
653 similar to one observed for saponite (Fig. 3) and talc (Čavajda et al. 2016) or Li-exchanged

montmorillonite heated above 300 °C (Derkowski and Kuligiewicz, in preparation). Further increase of this DTG peak intensity after isothermal heating for a longer time proves that after 4 h the binding is not complete, therefore, Mg-fixation is a relatively slow process in respect to dehydration or dehydroxylation.

The presence of cation-bound H_2O at temperatures corresponding to dehydroxylation could affect the E_a evolution in a course of dehydroxylation. Bonding of Mg^{2+} within theoctahedral sheet leads to the formation of a local trioctahedral arrangement of $AlMg_2OH$ and - much less abundant - Mg_3OH (Calvet and Prost 1971; Emmerich et al. 2001; Komadel 2005). An increase of structure heterogeneity that accompanies the migration of dehydrated Mg^{2+} cations into 2:1 layer seems to be the most probable explanation for a strong decrease in E_a of dehydroxylation of Mg-exchanged high-charge montmorillonites. The structural heterogeneity is then reflected in E_a evolution along with the degree of dehydroxylation, as predicted by Drits et al. (2012). Prolonged drying at temperatures above 110 °C is, therefore, not feasible for Mg-saturated montmorillonites, due to a potential structure alteration.

TBW removal in smectites *versus* zeolites

The H_2O/EXCH ratios in smectites and zeolites are in a remarkable agreement for the same drying temperature and interlayer cation type (Fig. 5). Furthermore, E_a of dehydration for Ca-exchanged smectites and zeolites, presented as a function of H_2O/EXCH, is in the same range, and displays similar trends, e.g., a gradual increase from 80-90 kJ/mol to reach 160-180 kJ/mol at H_2O/EXCH equal to 0.1 (Fig. 10). E_a values and evolution patterns obtained in the present study for Ca-13X and smectites are in accordance with those observed for the final stages of zeolite

dehydration found in other studies (Dondur and Vučelić 1983; Dima and Rees 1987; Yu et al. 1992). Significant similarities in the adsorbed water structure exist between smectites and low Si/Al zeolites i.e., 4A and 13X used in this study. In both systems, a fraction of water molecules is strongly bound in the first hydration spheres of the interlayer or extraframework cations while the remaining adsorbed water is a more mobile fraction in which H_2O-H_2O interactions dominate over cation-H_2O, so called "free water" (Bougard and Smirnov 2006). During zeolite dehydration, free water is removed first, with the remaining part held in the hydration spheres of the cations (Knowlton and White 1981), which is a very similar process to smectite dehydration (Bish 2006). Taking into account all similarities in H_2O/EXCH ratios and E_a of TBW removal between smectites and zeolites (Fig. 5, 9, and 11), the TBW content during final stages of dehydration has to be governed by the same factors in both systems, i.e., temperature and exchangeable cation hydration enthalpy, with little or no influence of the system geometry, despite significant differences in the latter. Apparently, the three dimensional diffusion in the pore structure of zeolites has a similar effect on the overall dehydration reaction kinetics as the two-dimensional diffusion in the collapsed interlayer space occurring during TBW removal in smectites (Ferrage et al. 2007b, Bray and Redfern 1999). The increased diffusion path tortuosity in the collapsed interlayer space of smectite makes it texturally similar to zeolitic channels rather than 2-dimensional diffusion.

The similarities in dehydration of smectites and zeolites allow using zeolites as an OH-free analog to estimate the conditions of complete TBW removal in smectites. Temperatures of final dehydration in Ca- and La- X and Y zeolites, between 550 and 600 °C (Costenoble et al. 1978) are in perfect agreement with TVD of SAP saturated with divalent cations (Table 4), where these values seem least affected by the dehydroxylation DTG peak (Fig. 3). Slightly lower

699 temperatures of dehydration completion, 400-500 °C, were found in A zeolites saturated with
700 divalent and monovalent cations of high hydration enthalpy in respect to K-saturated specie
701 where dehydration is finished at ~ 350 °C (Dondur and Vučelić 1983). A similarity to the results
702 found in smectites can also be tracked in a series of zeolite X saturated with monovalent cations
703 of different hydration enthalpy, from Cs to Li, where the completion of dehydration changes from
704 < 250C to 350 °C, respectively (Hunger et al. 1999). Synthetic samples, however, always contain
705 some post-synthesis impurities that can provide unexplained mass loss at a high temperature,
706 making the dehydration completion temperature difficult to identify from a TG curve (cf. Fig. 6
707 and 10).

708 In the absence of other effects, e.g., fixing within the 2:1 layer, the cations of a high
709 hydration enthalpy can hold water molecules to the temperatures corresponding to advanced
710 dehydroxylation in dioctahedral clay minerals (Fig. 3 and Table 2). The ability of holding H_2O to
711 temperatures as high as 600 °C by Mg^{2+} cations remains in agreement with the conclusions of
712 Čavajda et al. (2016) who studied milled talc by TG and IR methods.

713

714 **Implications**

715 Precise determination of the TBW contents and the conditions of the most complete TBW
716 removal strongly impacts the studies on stable O and H isotopes in smectites, as indicated by
717 Savin and Hsieh (1998), and demonstrated experimentally by Marumo et al. (1995), and Bauer
718 and Venneman (2013). For instance, in Mg-exchanged samples dried at 200 °C, for every water
719 molecule coming from structural OH, there is up to 1.0 tightly bound water molecules, which
720 translates to 50% of hydrogen present in the structure actually coming from TBW molecules, thus

721 having an isotopic signature of sample storing conditions and not the clay mineral formation
722 environment. δD measurement of such a sample would be heavily biased. Analogous calculations
723 for other samples dried at 200 °C returned values between 35 and 24%, 24 and 9, and 15 and 0,
724 for Ca-, Na-, and Cs-exchanged samples, respectively. Concluding, exchanging smectite with
725 monovalent cations of low hydration enthalpy (e.g., Cs or K; cf. Fig. 11) is a crucial pretreatment,
726 which, combined with in-situ drying to at least 200 °C (preferably 300 °C), allows minimizing
727 the effect of TBW contribution to the structural δD and – to a lesser extent – in the $\delta^{18}O$
728 measurements. The same recommendation is valid for smectite interstratified clays (e.g., illite-
729 smectite), where the proportion of TBW contribution is linear to the fraction of smectitic layers
730 (cf. Środon et al. 2009).

731 Quantification of TBW allows understanding the details of dehydroxylation and
732 rehydration of smectites, because a clear definition of initial "dry" state is required in those cases
733 (Derkowski et al. 2012b). Commonly used descriptive terms like "dehydrated" or "dry" may refer
734 to, as demonstrated, structures still containing considerable amounts of molecular water. Failure
735 to account for those molecules may lead to results misinterpretation, as even small amounts of
736 H_2O significantly alter bonding and layer charge distribution in the smectite structure (Xu et al.
737 2000; Rinnert et al. 2005; Schnetzer et al. 2016). Complete dehydration, however, may lead to
738 hardly-reversible alteration in the 2:1 layer structure, as presented for high-charge
739 montmorillonites (Kawano and Tomita 1989; Komadel et al. 2005). Finally, the proposed
740 approach of apparent E_a calculation can be used to differentiate between E_a of the dehydration (or
741 dehydration-dominated) domain and the dehydroxylation domain, although more work is
742 required to constrain the extent of overlap between these two processes.

743 Cationic, thermally stable zeolites were found as representing good models for TBW
744 evolution in smectites, following very similar properties of the residual water in both mineral
745 families. The results presented can also serve to develop an optimal strategy to minimize the
746 adsorbed water content in smectite- or illite-smectite -rich samples. Shales or soils are usually
747 considered "dehydrated" after extensive drying at 105 or 110 °C, which are the conditions
748 sufficient to remove the bulk interlayer water and a portion of H_2O from the cations' first
749 hydration shell, but only the increase of temperature, not time of drying, allows removal of the
750 residual, clay-bound water. An increase of the time of drying beyond certain values will not lead
751 to a decrease of TBW content at a given temperature. In the case of petrophysical analyses, the
752 TBW content would affect an estimation of a rock total and effective porosity and the mineral
753 matrix grain density (Topór et al. 2016). If possible, exchanging a sample with a cation of low
754 hydration enthalpy, such as Cs^+, is recommended (cf. Fig. 11). Drying at 300 °C leads to the most
755 complete dehydration of a sample, however, due to potential dehydroxylation of Fe-rich clay or
756 decomposition of organic matter usually present in rocks and soils, using the temperature not
757 higher than 200 °C is recommended (Środon and McCarty 2008; Derkowski and Marynowski
758 2016; Topór et al. 2016).

759 If there is no cation migration into the 2:1 layer structure, H_2O molecules are bound to
760 cations of a high hydration enthalpy (i.e., Mg^{2+}) tightly enough, so that they can be carried to the
761 temperatures corresponding to dehydroxylation. In geologic systems such conditions correspond
762 to those above common smectite dehydration under sedimentary conditions (Brown and Ransom
763 1996). Besides the OH groups in clays, TBW in smectite and smectite interstratified clays can be
764 a non-negligible source of hydrogen and molecular H_2O introduced into Earths' crust, e.g., by
765 subduction (Vrolijk 1990). Most likely some TBW can add to the H_2O formed by clay

766 dehydroxylation during earthquakes, which affects faults propagation (cf., Hirono and Tanikawa
767 2011).

768 **Acknowledgements**

769 The authors thank Małgorzata Lempart and Tomasz Topór for technical assistance. Marek
770 Szczerba is acknowledged for his essential comments. The authors thank Javier Cuadros and one
771 anonymous reviewer for their comments that greatly helped in improving the manuscript. The
772 study was funded by IGS-PAS internal research grant for young researchers. This work was
773 performed to partially fulfill the requirements of a PhD thesis by A. Kuligiewicz.

Literature

Bauer, K.K., Vennemann, T.W. (2013) Analytical methods for the measurement of hydrogen isotope composition and water content in clay minerals by TC/EA. Chemical Geology, 363, 229-240.

Bérend, I., Cases, J.M., François, M., Uriot, J.P., Michot, L., Masion, A., and Thomas, F. (1995) Mechanism of adsorption and desorption of water-vapor by homoionic montmorillonites: 2. The Li^+, Na^+, K^+, Rb^+ and Cs^+-exchanged forms. Clays and Clay Minerals, 43, 324-336.

Bish, D.L. (2006) Parallels and distinctions between clay minerals and zeolites. In F. Bergaya, B.K.G. Theng, and G. Lagaly, Ed., Handbook of Clay Science, p. 1097-1112, Elsevier, Netherlands.

Bougeard, D., Smirnov, C. (2007) Modelling studies of water in crystalline nanoporous aluminosilicates. Physical Chemistry Chemical Physics, 9, 226-245.

Bray, H.J., Redfern, S.A.T. (1999) Kinetics of dehydration of Ca-montmorillonite. Physics and Chemistry of Minerals, 26, 591-600.

Bray, H.J., Redfern, S.A.T. (2000) Influence of counterion species on dehydroxylation of Ca^{2+}-, Mg^{2+}-, Na^+- and K^+-exchanged Wyoming montmorillonite. Mineralogical Magazine, 64, 337-346.

Brown, K.M., and Ranson B. (1996) Porosity corrections for smectite-rich sediments: Impact on studies of compaction, fluid generation, and tectonic history. Geology, 24, 843-846.

Calvet, R., Prost, R. (1971) Cation migration into empty octahedral sites and surface properties of clays. Clays and Clay Minerals, 19, 175-186.

Cases, J.M., Bérend, I., Besson, G., François, M., Uriot, J.P., Thomas, E., and Poirier, J.R. (1992) Mechanism of adsorption-desorption of water vapor by homoionic montmorillonite. 1. The sodium exchanged form. Langmuir, 8, 2730-2739.

Cases, J.M., Bérend, I., François, M., Uriot, J.P., Michot, L.J., and Thomas, F. (1997) Mechanism of adsorption and desorption of water vapor by homoionic montmorillonite: 3. The Mg^{2+}, Ca^{2+}, Sr^{2+} and Ba^{2+} exchanged forms. Clays and Clay Minerals, 45, 8-22.

Čavajda, V., Uhlík, P., Derkowski, A., Čaplovičová, M., Madejová, J., Mikula, M., Ifka, T. (2015) Influence of grinding and sonication on the crystal structure of talc. Clays and Clay Minerals, 63, 311-327.

Chiou, C.T., and Rutherford, D.W. (1997) Effects of exchanged cation and layer charge on the sorption of water and EGME vapors on montmorillonite clays. Clays and Clay Minerals, 45, 867-880.

Costenoble, M., Mortier, W.J., and Uytterhoeven, J.B. (1978) Location of cations in synthetic zeolites-X and -Y. Part 5. The cation distribution in Ca-Y, Ca-X and La-Y in the ultimate stages of dehydration. Journal of the Chemical Society, Faraday Transactions 1: Physical Chemistry in Condensed Phases, 74, 466-476.

Criado, J.M., Sánchez-Jiménez, P.E., and Pérez-Maqueda, L.A. (2007) Critical study of the isoconversional methods of kinetic analysis. Journal of Thermal Analysis and Calorimetry, 92, 199-203.

Cuadros, J. (1997) Interlayer cation effects on the hydration state of smectite. American Journal of Science, 297, 829-841.

Cuadros, J., Huertas, F., Delgado, A., and Linares, J. (1994a) Determination of hydration (H_2O^-) and structural (H_2O^+) water for chemical analysis of smectites. Application to Los Trancos smectites, Spain. Clay Minerals, 29, 297-300.

Cuadros, J., Delgado, A., Cardenete, A., Reyes, E., and Linares, J. (1994b) Kaolinite/montmorillonite resembles beidellite. Clays and Clay Minerals, 5, 643-651.

Derkowski, A., and Marynowski, L. (2016) Reactivation of cation exchange properties in black shales. International Journal of Coal Geology, 158, 65-77.

Derkowski, A., Franus, W., Waniak-Nowicka H., and Czímerová, A. (2007) Textural properties vs. CEC and EGME retention of Na–X zeolite prepared from fly ash at room temperature International Journal of Mineralogical Processing 82, 57–68

Derkowski, A., Drits, V.A., and McCarty, D.K. (2012a) Nature of rehydroxylation in dioctahedral 2:1 layer clay minerals. American Mineralogist, 97, 610-629.

Derkowski, A., Drits, V.A., and McCarty, D.K. (2012b) Rehydration of dehydrated-dehydroxylated smectite in a low water vapor environment. American Mineralogist, 97, 110-127.

Dima, E., and Rees, V.C. (1987) Temperature programmed desorption of sorbates from zeolites: Part 2. New analytical method tested on dehydration of dealuminated Y zeolites. Zeolites, 7, 219-277.

Ding, Z., and Frost, R.L. (2002) Controlled rate thermal analysis of nontronite. Thermochimica Acta, 389, 185-193.

Dondur, V., and Vučelić, D. (1983) An approach to the kinetics of water desorption from A-zeolites. Part II. Resolution of the complex dehydration process to elementary reactions. Thermochimica Acta, 68, 101-111.

Drits, V.A., Besson, G., and Muller, F. (1995) An improved model for structural transformations of heat-treated aluminous dioctahedral 2:1 layer silicates. Clays and Clay Minerals, 43, 718-731.

Drits, V.A., Derkowski, A., and McCarty, D.K. (2012) Kinetics of partial dehydroxylation in dioctahedral 2:1 layer clay minerals. American Mineralogist, 97, 930-950.

Dudek, T., Cuadros, J., and Fiore, S. (2006) Interstratified kaolinite-smectite: Nature of the layers and mechanism of smectite kaolinization. American Mineralogist, 91, 159-170.

El-Barawy, K., Girgis, B., Felix, N. (1986) Thermal treatment of some pure smectites. Thermochimica Acta, 98, 181-189.

Emmerich, K., Madsen F.T., and Kahr G. (1999) Dehydroxylation behavior of heat-treated and steam-treated homoionic cis-vacant montmorillonites. Clays and Clay Minerals, 47, 591-604.

Emmerich, K., Plötze, M., Kahr, G. (2001) Reversible collapse and Mg^{2+} release of de- and rehydroxylated homoionic *cis*-vacant montmorillonites. Applied Clay Science, 9, 143-154.

Ferrage, E., Kirk, C.A., Cressey, G., and Cuadros, J. (2007a) Dehydration of Ca-montmorillonite at the crystal scale. Part I: Structure evolution. American Mineralogist, 92, 994-1006.

Ferrage, E., Kirk, C.A., Cressey, G., and Cuadros, J. (2007b) Dehydration of Ca-montmorillonite at the crystal scale. Part 2. Mechanisms and kinetics. American Mineralogist, 92, 1007-1017.

Ferrage, E., Lanson, B., Sakharov, B.A., Geoffroy, N., Jacquot, E., and Drits, V.A. (2007c) Investigation of dioctahedral smectite hydration properties by modeling of X-ray diffraction profiles: Influence of layer charge and charge location. American Mineralogist, 92, 1731-1743.

Ferrage, E., Lanson, B., Michot, L.J., and Robert, J-L. (2010) Hydration Properties and Interlayer Organization of Water and Ions in Synthetic Na-Smectite with Tetrahedral Layer Charge. Part 1. Results from X-ray Diffraction Profile Modeling. Journal of Physical Chemistry C, 114, 4515-4526.

Frost, R.L., Ruan, H., Kloprogge, J.T., and Gates, W.P. (2000) Dehydration and dehydroxylation of nontronites and ferruginous smectite. Thermochimica Acta, 346, 63-72.

Girgis, B.S., El-Barawy, K.A., and Felix, N.S. (1987) Dehydration kinetics of some smectites: A thermogravimetric study. Termochimica Acta, 111, 9-19.

Hirono, T., and Tanikawa, W. (2011) Implications of the thermal properties and kinetic parameters of dehydroxylation of mica minerals for fault weakening, frictional heating, and earthquake energetic. Earth and Planetary Science Letters, 307, 161-172.

Hunger, B., Klepel, O., Kirschhock, C., Heuchel, M., Toufar, H., and Fuess, H. (1999) Interaction of water with alkali-metal cation-exchanged X type zeolites: A temperature-programmed desorption (TPD) and X-ray diffraction study. Langmuir, 15, 5937-5941.

Jackson, M.L. (1969) Soil Chemical Analysis: Advanced Course, 895 p. Published by the author.

Kawano, M., and Tomita, K. (1989) X-ray studies of rehydratation behaviors for montmorillonite. Clay Science, 7, 277-287.

874 Kawano, M., and Tomita, K. (1991) X-ray-powder diffraction studies on the rehydration
875 properties of beidellite. Clays and Clay Minerals, 39, 77-83.

876 Kaufhold, S., and Dohrmann, R. (2010) Effect of extensive drying on the cation exchange
877 capacity of bentonites. Clay Minerals, 45, 441-448.

878 Knowlton, G.D., White T.R., and MgKague, H.L. (1981) Thermal study of types of water
879 associated with clinoptiolite. Clays and Clay Minerals, 29, 403-411.

880 Kloprogge, J.T., Jansen, J.B.H., Schuiling, R.D., and Geus, J.W. (1992) The interlayer collapse
881 during dehydration of synthetic $Na_{0.7}$-beidellite: A ^{23}Na solid-state magic-angle spinning NMR
882 study. Clays and Clay Minerals, 40, 561-566.

883 Komadel, P., Madejová, J., and Bujdák, J. (2005) Preparation and properties of reduced-charge
884 smectites – a review. Clays and Clay Minerals, 53, 313-334.

885 Kuligiewicz, A., Derkowski, A., Szczerba, M., Gionis, V., and Chryssikos, G.D. (2015)
886 Revisiting the infrared spectrum of the water-smectite interface. Clays and Clay Minerals, 63, 15-
887 29.

888 Marcus, Y. (1994) A simple empirical model describing the thermodynamics of hydration of ions
889 of widely varying charges, sizes and, shapes. Biophysical Chemistry, 2-3, 111-127.

890 Marumo, K., Longstaffe, F.J., and Matsubaya, O. (1995) Stable isotope geochemistry of clay
891 minerals from fossil and active hydrothermal systems, southwestern Hokkaido, Japan.
892 Geochimica et Cosmochimica Acta, 59, 2545-2559.

893 Merchant, S., and Asthagiri, A. (2009) Thermodynamically dominant hydration structures of
894 aqueous ions. The Journal of Chemical Physics, 130, 195102.

895 Michot, L.J., Bihannic, I., Pelletier, M., Rinnert, E., and Robert, J-L. (2005) Hydration and
896 swelling of synthetic Na-saponites: Influence of layer charge. American Mineralogist, 90, 166-
897 172.

McCarty, D.K., Theologou, P.N., Fischer, T.B., Derkowski, A., Stokes, M.R., and Ollila, A. (2015) Mineral-chemistry quantification and petrophysical calibration for multimineral evaluations: A nonlinear approach. AAPG Bulletin, 99, 1371-1397.

Mooney, R.W., Keenan, A.G., and Wood, L.A. (1952) Adsorption of water vapor by montmorillonite. II. Effect of exchangeable ions and lattice swelling as measured by X-ray diffraction. Journal of the American Chemical Society, 74, 1371-1374.

Pavlov, M., Siegbahn, P.E.M., Sandström, M. (1998) Hydration of beryllium, magnesium, calcium, and zinc ions using density functional theory. Journal of Physical Chemistry A, 102, 219-228.

Pelletier, M., Michot, L.J., Humbert, B., Barrès, O., de la Caillerie, J.B.D., and Robert, J-L. (2003) Influence of layer charge on the hydroxyl stretching of trioctahedral clay minerals: A vibrational study of synthetic Na- and K-saponites. American Mineralogist, 88, 1801-1808.

Poinsignion, C., Yvon, J., and Mercier, R. (1982) Dehydration energy of the exchangeable cations in montmorillonite - a DTA Study. Israel Journal of Chemistry, 22, 253-255.

Prado J.R., and Vyazovkin, S. (2011) Activation energies of water vaporization from the bulk and from laponite, montmorillonite, and chitosan powders. Thermochimica Acta, 524, 197-201.

Rinnert, E., Carteret, C., Humbert, B., Fragneto-Cusani, G., Ramsay, J.D.F., Delville, A., Robert, J-L., Bihannic, I., Pelletier, M., and Michot, L.J. (2005) Hydration of a synthetic clay with tetrahedral charges: A multidisciplinary experimental and numerical study. Journal of Physical Chemistry B, 109, 23745-23759.

Sato, T., Watanabe, T., and Otsuka, R. (1992) Effects of layer charge, charge location, and energy change on expansion properties of dioctahedral smectites. Clays and Clay Minerals, 40, 103-113.

Savin, S.M., and Hsieh, J.C.C. (1998) The hydrogen and oxygen isotope geochemistry of pedogenic clay minerals: Principles and theoretical background. Geoderma, 82, 227-253.

924 Schnetzer, F., Thissen, P., Giraudo, N., and Emmerich, K. (2016) Unraveling the coupled
925 processes of (de)hydration and structural changes in Na^{+}-saturated montmorillonite. The Journal
926 of Physical Chemistry C, 120, 15282-15287.

927 Steudel, A., and Emmerich, K. (2013) Strategies for the successful preparation of homoionic
928 smectites. Applied Clay Science, 75-76, 13-21.

929 Środoń, J., and McCarty, D.K. (2008) Surface area and layer charge of smectite from CEC and
930 EGME/H2O-retention measurements. Clays and Clay Minerals, 56, 155-174.

931 Środoń, J., Zeelmaekers, E., and Derkowski, A. (2009) The charge of component layers of illite-
932 smectite in bentonites and the nature of end-member illite. Clays and Clay Minerals, 57, 649-671.

933 Topór, T., Derkowski, A., Kuila, U., Fischer, T.B., and McCarty D.K. (2016) Dual liquid
934 porosimetry: porosity measurement method for oil and gas bearing shales. Fuel, 183, 537–549.

935 Wolters, F., and Emmerich, K. (2007) Thermal reactions of smectites – Relations of
936 dehydroxylation temperature to octahedral structure. Thermochimica Acta, 462, 80-88.

937 Xu, W., Johnston, C.T., Parker, P., and Agnew, S.F. (2000) Infrared study of water sorption on
938 Na-, Li-, Ca- and Mg-exchanged (SWy-1 and SAz-1) montmorillonite. Clays and Clay Minerals,
939 48, 120-131.

940 Vrolijk, P. (1990) On the mechanical role of smectite in subduction zones. Geology, 18, 703-707.

941 Vyazovkin, S., Burnham, A.R., Criado, J.M., Pérez-Maqueda, L.A., Popescu, C., Sbirrazzuoli, N.
942 (2011), ICTAC Kinetics Committee recommendations for performing kinetic computations on
943 thermal analysis data. Thermochimica Acta, 520, 1-19.

944 Yu, B.L., Dyer, A., and Enamy, H. (1992) A thermoanalytical study of the dehydration of NaA,
945 MgNaA, CaNaA and SrNaA zeolites. Thermochimica Acta, 200, 299-308.

946 Zabat, M., and Van Damme, H. (2000) Evaluation of the energy barrier for dehydration of
947 homoionic (Li, Na, Cs, Mg, Ca, Ba, $Al_x(OH)_z^{y+}$ and La)-montmorillonite by a differentiation
948 method. Clay Minerals, 35, 357-363.

Figure Captions

Figure 1. Examples of TG curves from SIH (a) and MIH (b) experiments for a Ca-SCa-3 sample: EI-110C4H-SIH – point at the end of isothermal heating segment in SIH experiment; EI-110-MIH, EI-200-MIH, EI-300-MIH – points at the end of 110, 200, and 300 °C isothermal heating segments, respectively, in a MIH experiment; EP – end point of the experiment; Δm_{DX} mass loss of dehydroxylation (cf. Table1); Δm_{exp} – mass differences measured between the end of isothermal heating segment and EP; TBW% - tightly-bound water content; TVD – temperature of virtual onset of dehydroxylation. See the text for further details. TBW contents are not to scale.

Figure 2. DTG curves from 200C4H-SIH experiments for Cs-SWy-2 and Cs-SWa-1 samples with a corresponding mass spectrometer (MS) signal of m/z 18 amu coming from the evolved H_2O and 44 amu, originating from evolved CO_2. The MS signal is not in scale between the two samples.

Figure 3. DTG curves for selected representative xC4H-SIH and xC12H-SIH experiments. A dot on a DTG curve marks the temperature of virtual onset of dehydroxylation (TVD; in °C).

Figure 4. The evolution of TBW content along with time for selected SIH and MIH experiments with the SAz-2 sample. Negative TBW values correspond to dehydroxylation.

Figure 5. The ratio of water molecules per interlayer cation (H_2O/EXCH; mol/mol) for SIH and MIH as a function of drying temperature, and the interlayer cation. Negative TBW values correspond to dehydroxylation.

Figure 6. DTG curves of SIH experiments with xC4H of 4A and 13X zeolites in Na^+ form. Small mass loss above 800 °C for 4A zeolites was ascribed to decomposition of residue after synthesis.

Figure 7. Kinetic data for ramp-heating segments of the experiments with isothermal heating segment for Friedman and KAS methods for the Mg-SCa-3 sample. Trend lines are for the points separated by 0.1 degree of reaction (α), starting at α=0.1 and are shown only for the points with R^2>0.9900.

Figure 8. The evolution of E_a along with dehydration for SAz-2, SCa-3, and SWy-2 samples in the experiments without isothermal preheating segment. H_2O/EXCH – number of water molecules per interlayer cation (mol/mol). The temperature curve corresponds to the heating rate of 5 °C/min. The number of water molecules in the first hydration sphere of Na^+ and Ca^{2+} after Michot et al. (2005) and Ferrage et al. (2007a), respectively. The number of water molecules for structural rearrangement of molecules around Ca^{2+} cation after Ferrage et al. (2007a,b).

Figure 9. Changes of the apparent E_a during progressive mass loss enclosing the range of TBW removal and the dehydroxylation region in the experiments involving the initial isothermal heating segment. The temperature curve corresponds to the heating rate of 5 °C/min.

Figure 10. Evolution of E_a along with molecular water removal for Ca-exchanged zeolite 13X and the SCa-3 smectite reference sample.

Figure 11. The relationship between the H_2O/EXCH ratio and the counterion hydration enthalpy in xC4H-SIH for smectites, and zeolites. Hydration enthalpies after Marcus (1994). Solid lines represent exponential fits for SAz-2 and SWy-2 samples.

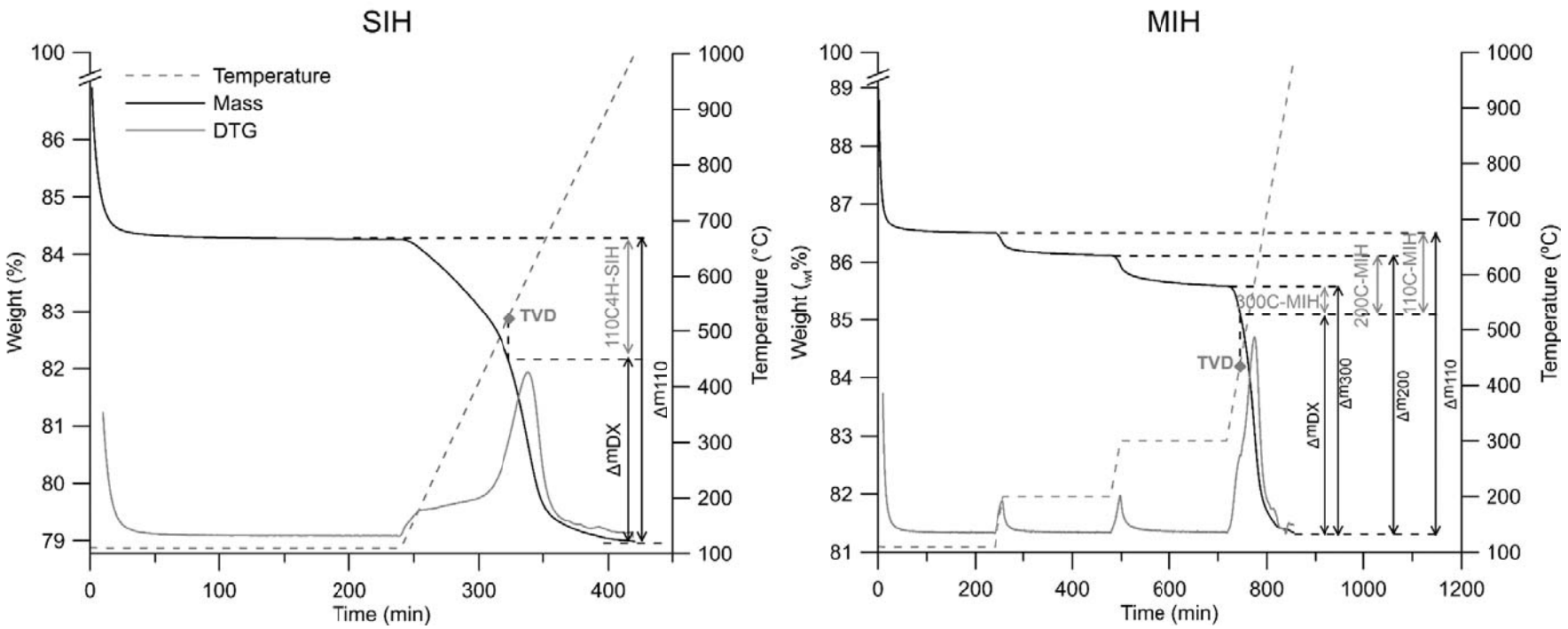
SIH
Temperature
Mass
DTG
Weight (%)
Temperature (°C)
Time (min)
TVD
110C4H-SIH
ΔmDX
Δm110
MIH
Weight (wt.%)
300C-MIH
200C-MIH
110C-MIH
Δm300
Δm200

Figure 1.

This is a preprint, the final version is subject to change, of the American Mineralogist (MSA)
Cite as Authors (Year) Title. American Mineralogist, in press.
(DOI will not work until issue is live.) DOI: http://dx.doi.org/10.2138/am-2017-5918

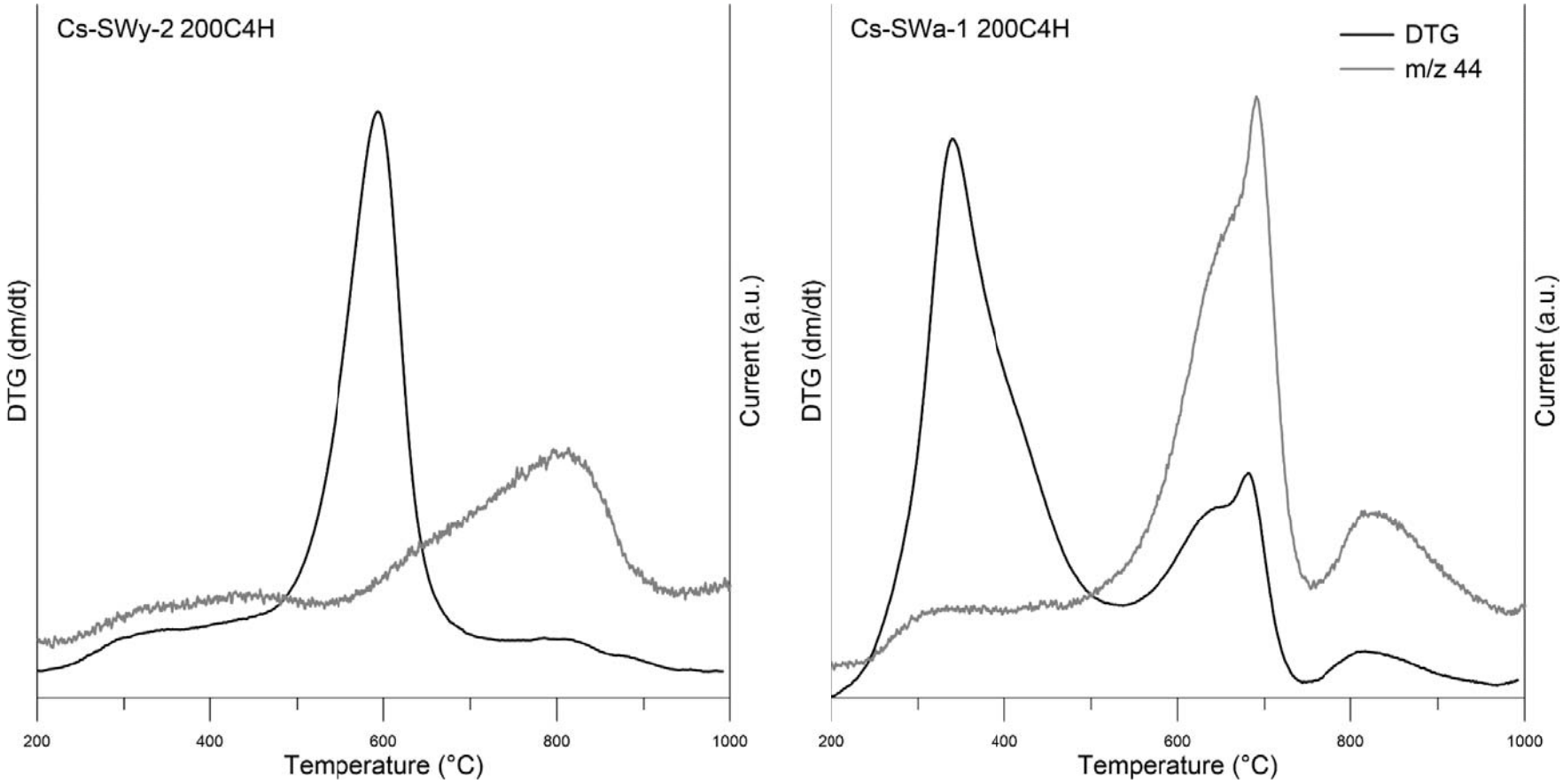

912

913 Figure 2.

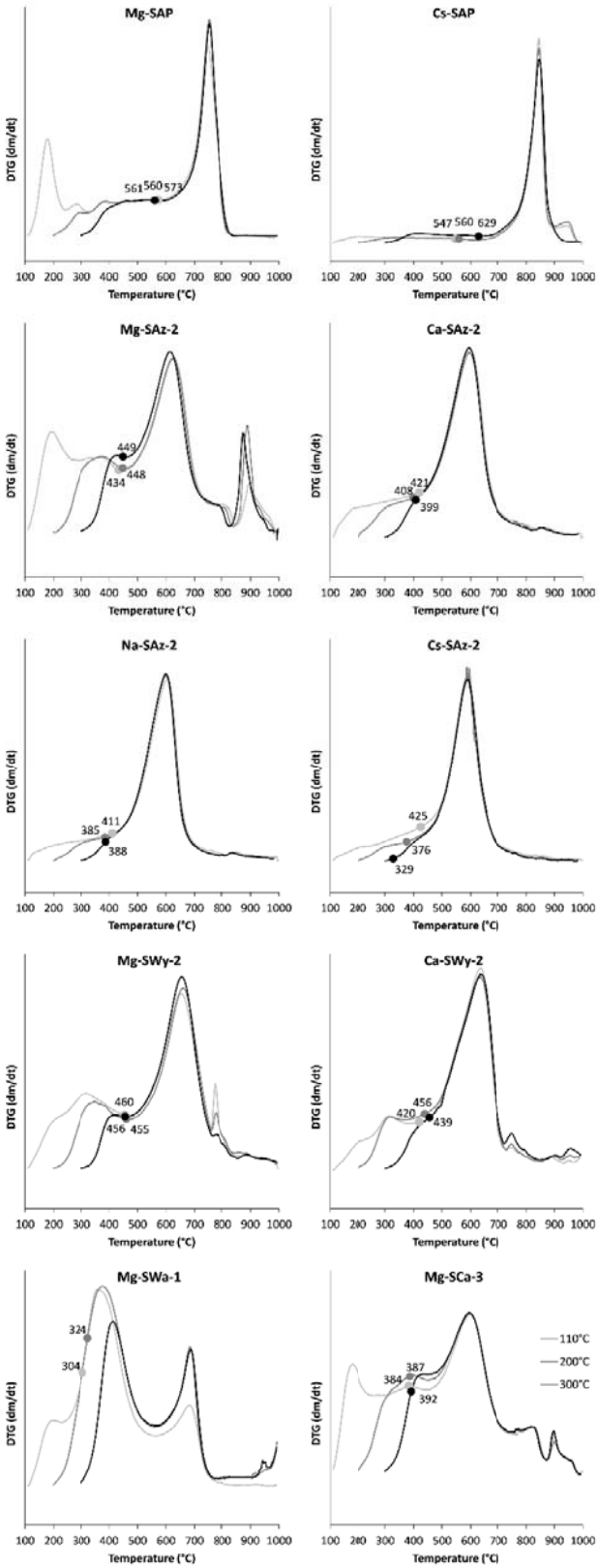

914

915 Figure 3.

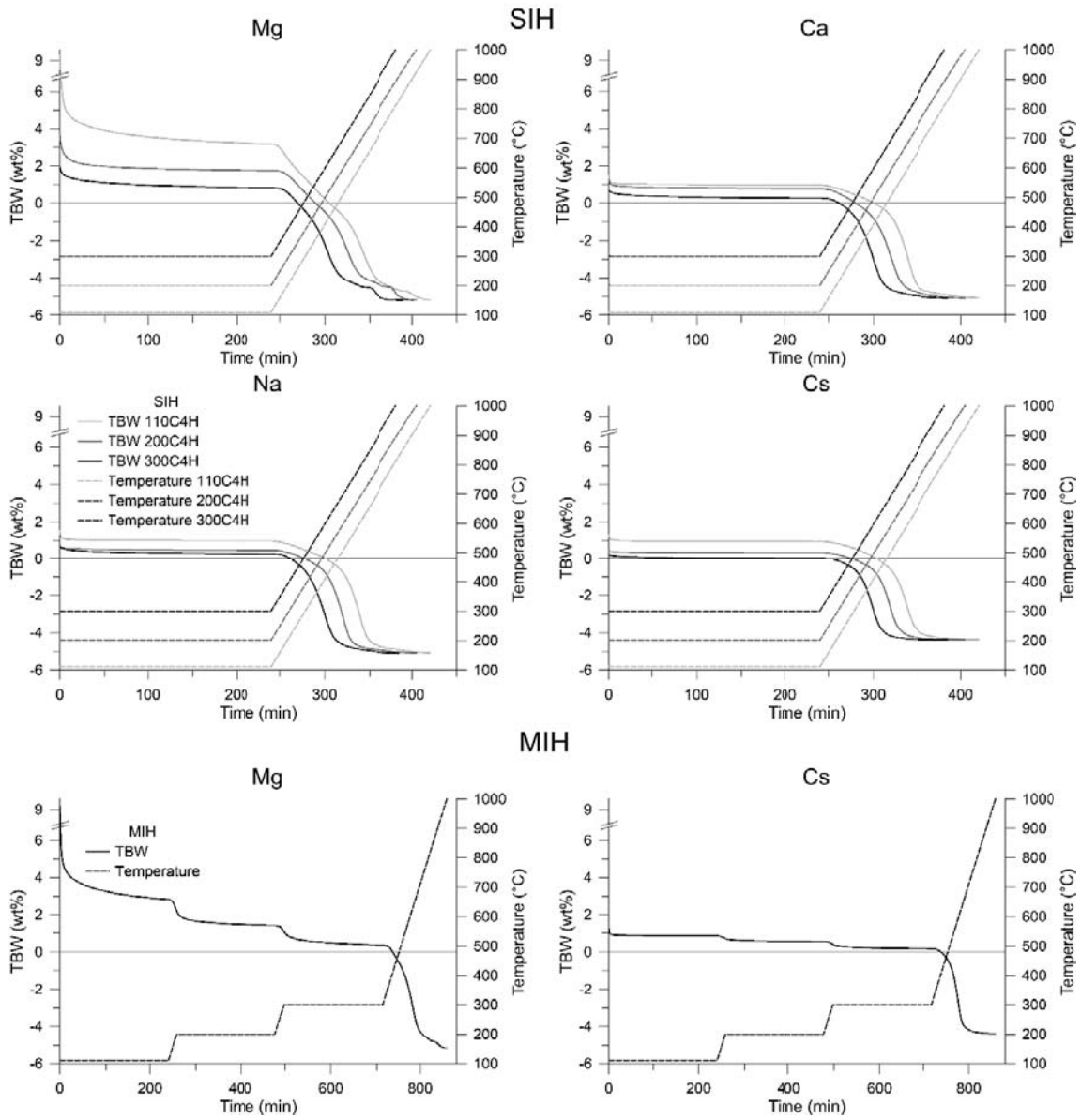

Figure 4.

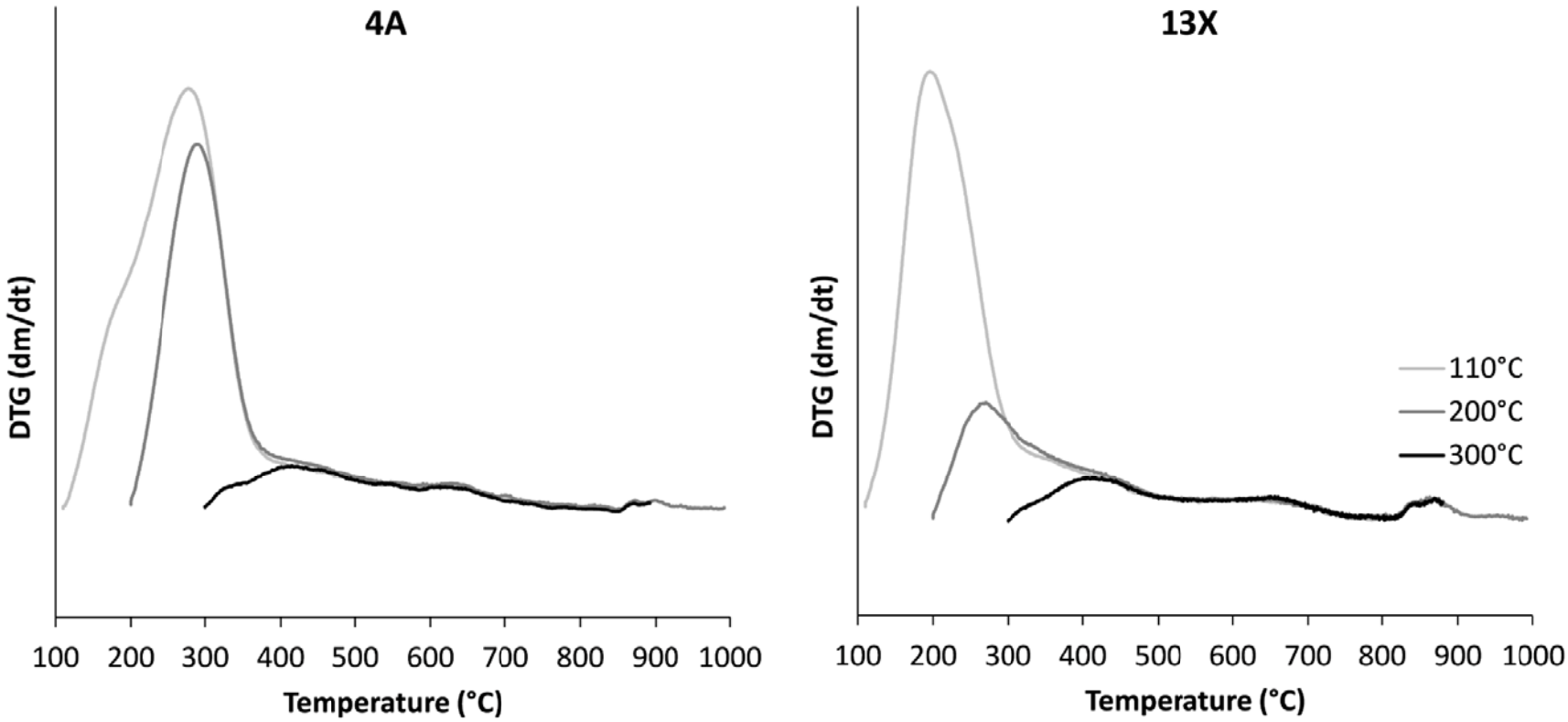

Figure 5.

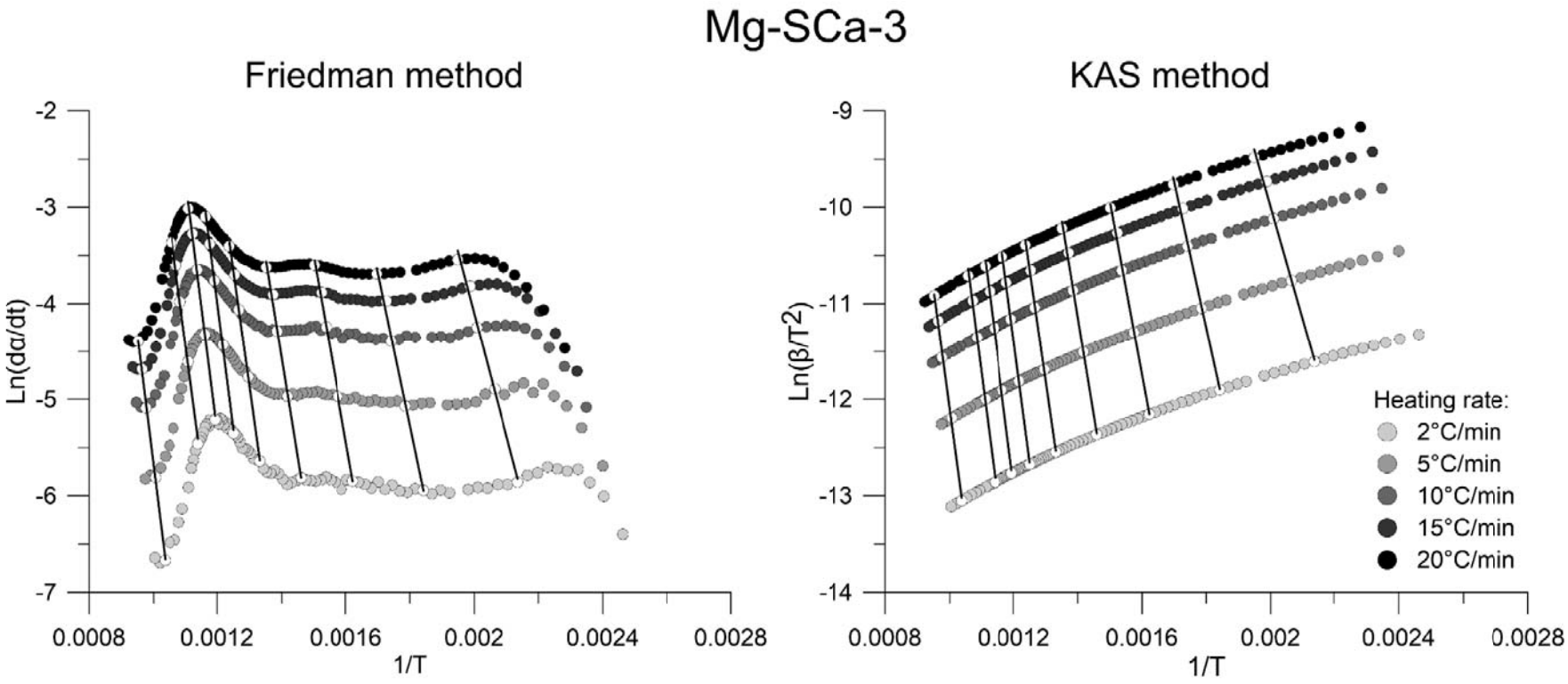
Mg-SCa-3
Friedman method
KAS method
Ln(dα/dt)
Ln(β/T2)
1/T
1/T
Heating rate:
2°C/min
5°C/min
10°C/min
15°C/min
20°C/min

Figure 6.

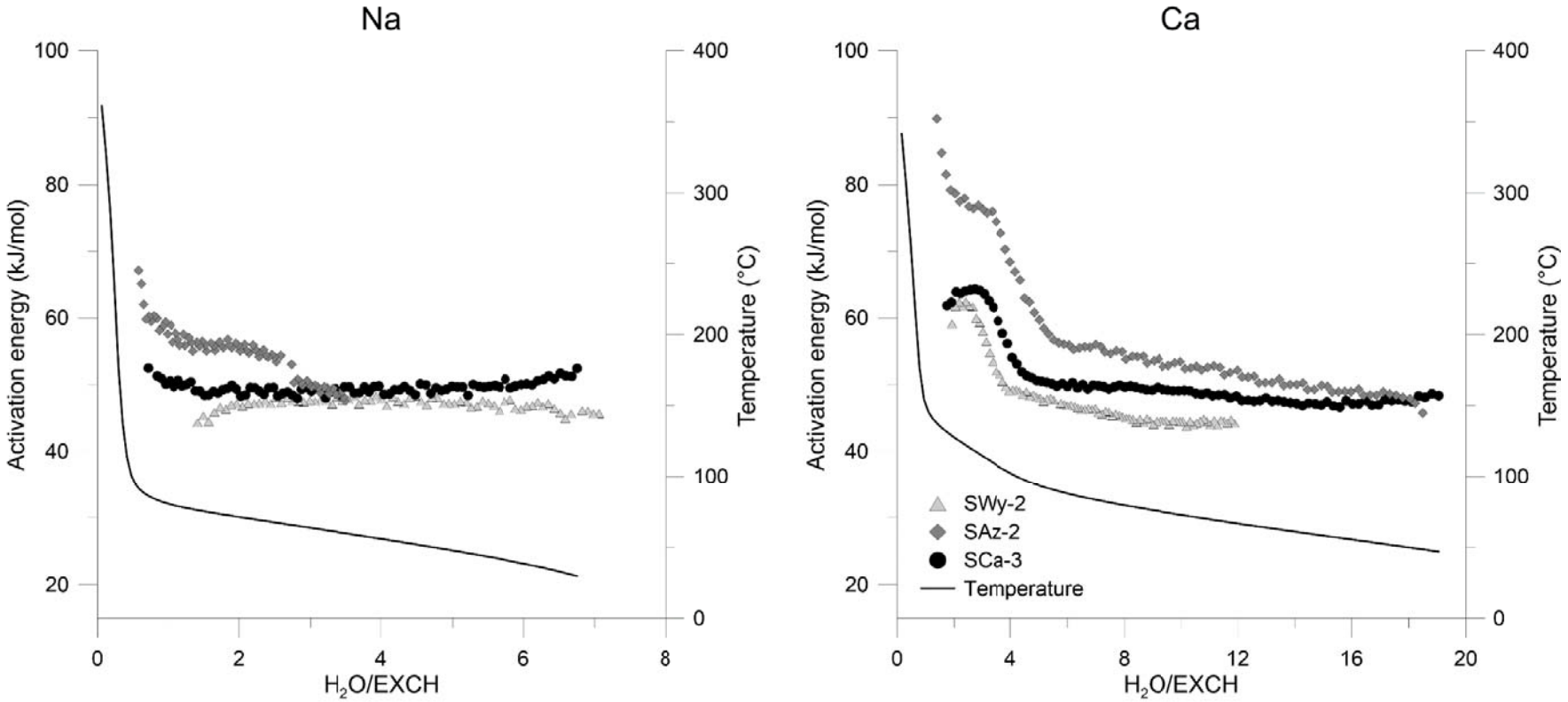
Na
Ca
Activation energy (kJ/mol)
Temperature (°C)
H2O/EXCH
SWy-2
SAz-2
SCa-3
Temperature

Figure 7.

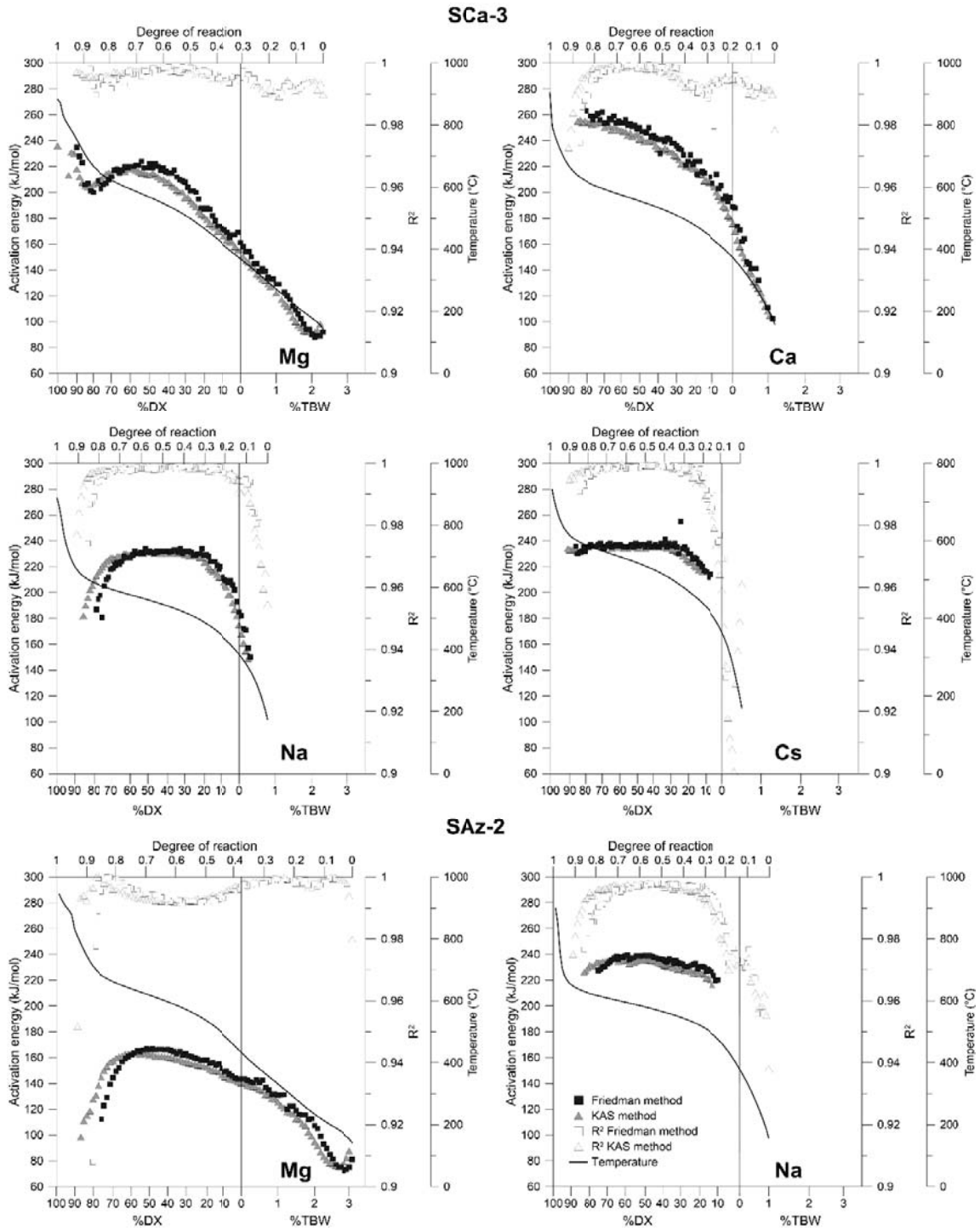

Figure 8.

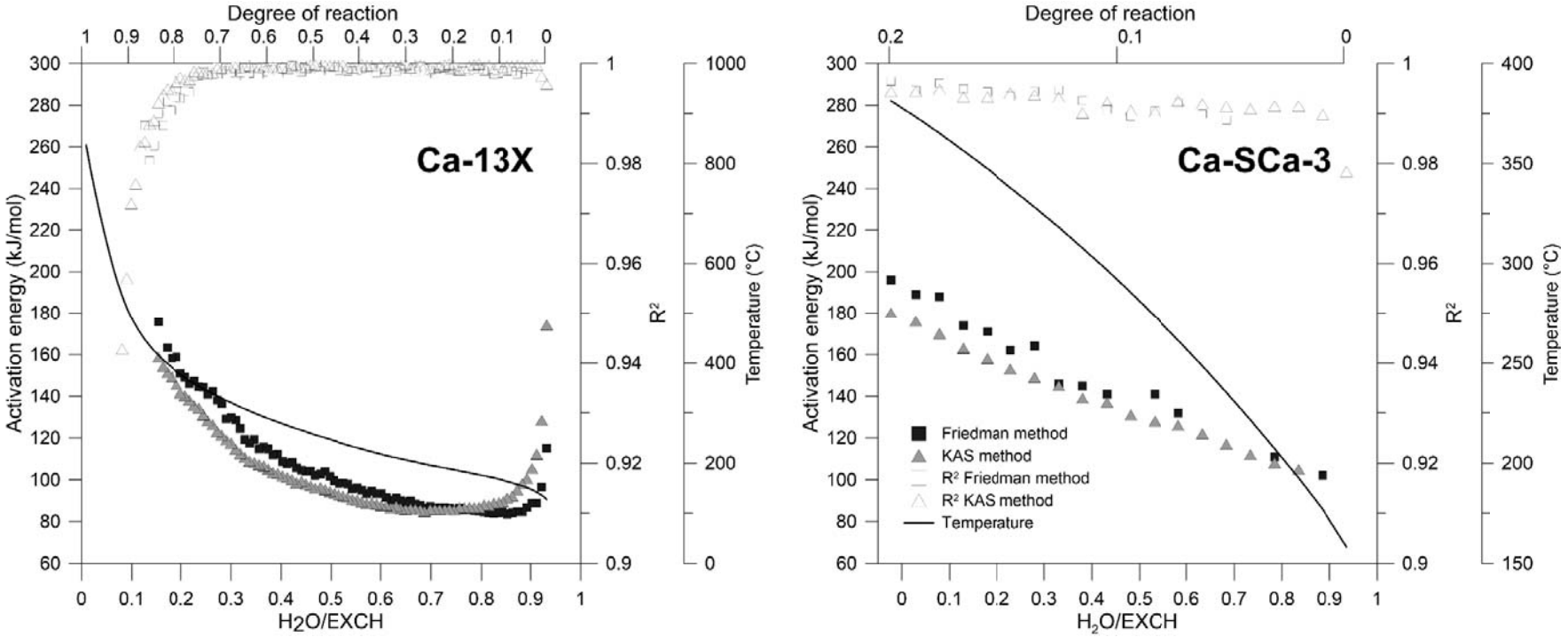

928

929 Figure 9.

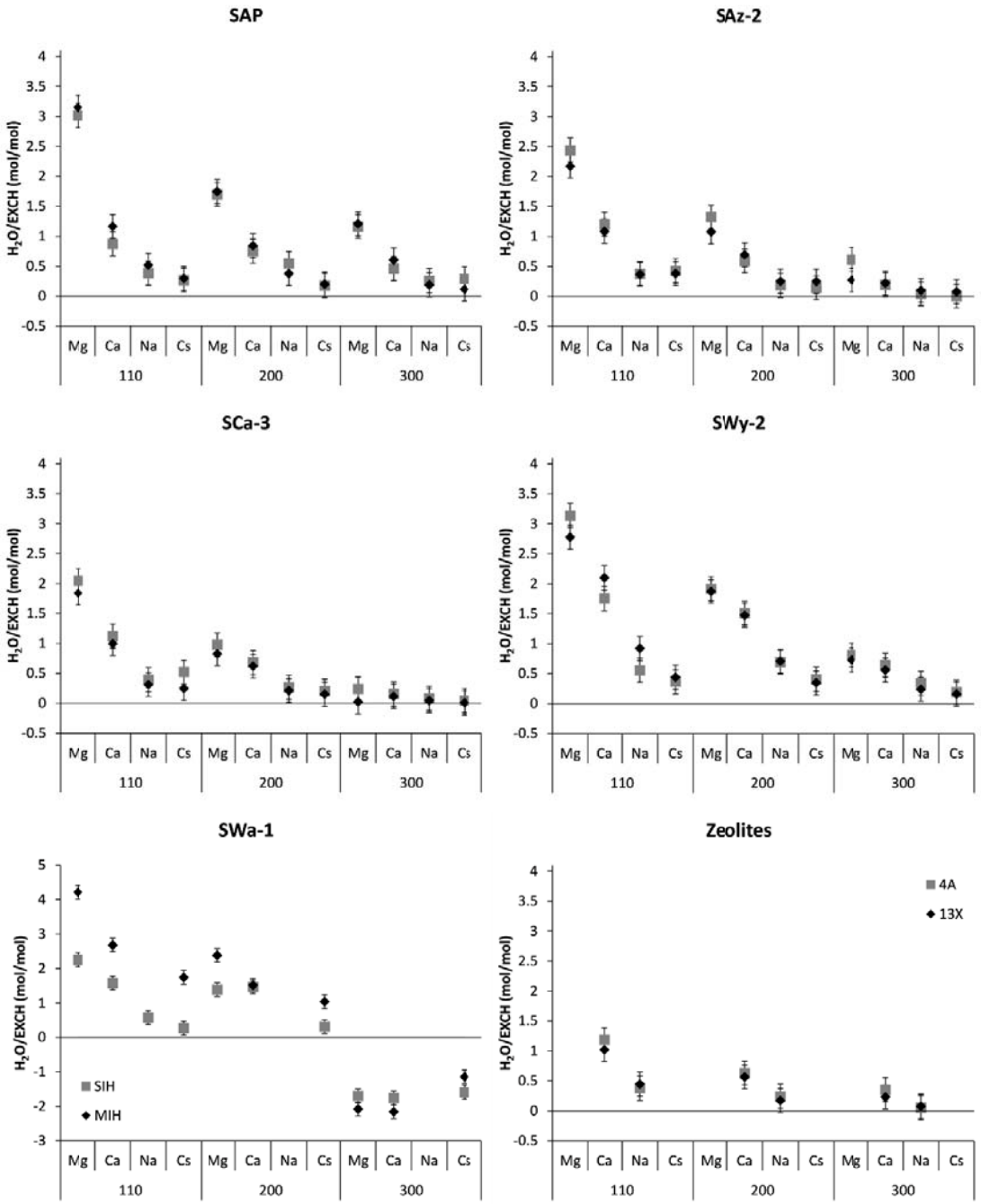

930

931 Figure 10.

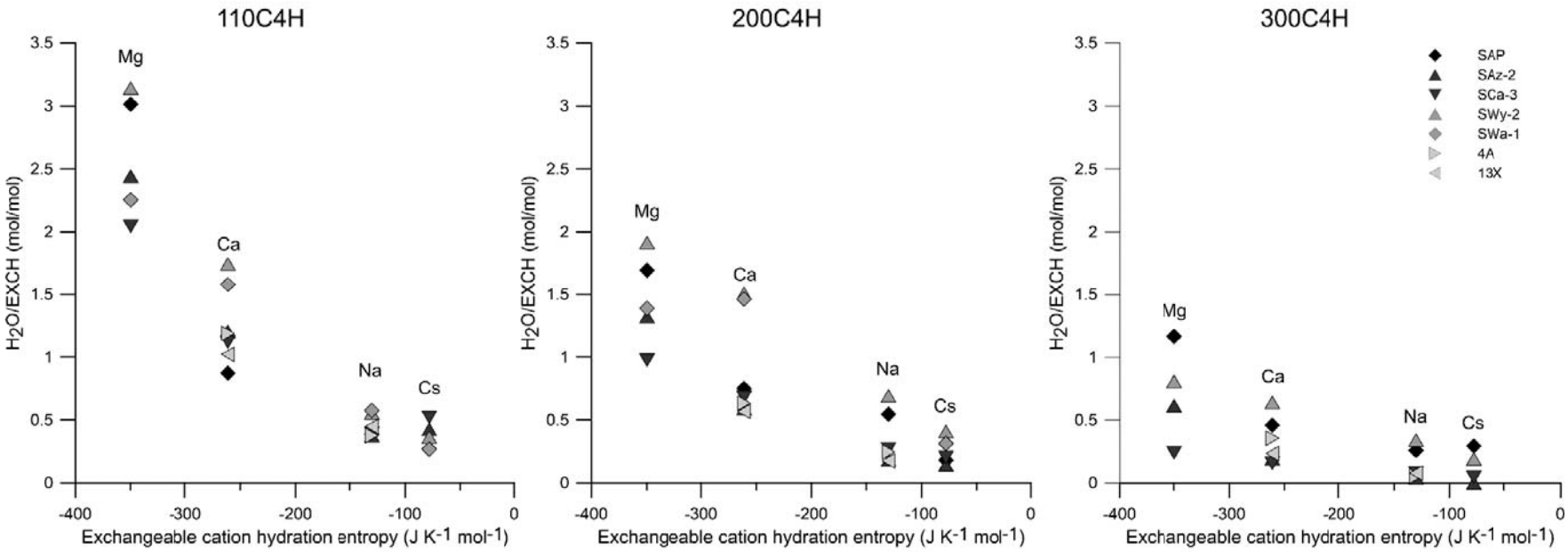

932

933 Figure 11.

This is a preprint, the final version is subject to change, of the American Mineralogist (MSA)
Cite as Authors (Year) Title. American Mineralogist, in press.
(DOI will not work until issue is live.) DOI: http://dx.doi.org/10.2138/am-2017-5918

993

994 Table 1. Samples used in the study.

Sample	Smectite octahedral structure	Octahedral vacancy type	Size fraction (μm)	Structural formula[a]	Theoretical mass loss upon dehydroxylation (Δm_{DX}) (%)[b]			
					Interlayer cation			
					Mg	Ca	Na	Cs
SAP	Trioctahedral	-	<2.0	$M^{+}_{0.58}(Si_{3.42}Al_{0.58})(Mg_3)O_{10}(OH)_2$	4.89	4.83	4.81	4.11
SAz-2	Dioctahedral	tv?	<2.0	$M^{+}_{0.52}(Al_{1.38}Mg_{0.52}Fe(III)_{0.07})(Si_4)O_{10}(OH)_2$	5.17	5.11	5.08	4.38
SCa-3		tv?	<1.0	$M^{+}_{0.51}(Al_{1.43}Mg_{0.49}Fe(III)_{0.08})(Si_{3.98}Al_{0.02})O_{10}(OH)_2$	5.15	5.09	5.07	4.38
SWy-2		cv	<0.1	$M^{+}_{0.36}(Al_{1.53}Mg_{0.24}Fe(III)_{0.23})(Si_{3.88}Al_{0.12})O_{10}(OH)_2$	5.11	5.06	5.05	4.54
SWa-1		tv	<1.0	$M^{+}_{0.31}(Al_{0.67}Mg_{0.07}Fe(III)_{1.26})(Si_{3.76}Al_{0.24})O_{10}(OH)_2$	4.71	4.68	4.67	4.29

995 [a] Structural formulae were adapted after Pelletier et al. (2003) for SAP and Derkowski et al. (2012b) with corrections by Kuligiewicz et al. (2015)
996 for the remaining samples.
997 [b] Normalized to mass of dehydroxylated structural formula.
998

999

This is a preprint, the final version is subject to change, of the American Mineralogist (MSA)
Cite as Authors (Year) Title. American Mineralogist, in press.
(DOI will not work until issue is live.) DOI: http://dx.doi.org/10.2138/am-2017-5918

1000 Table 2, TBW contents in wt% in the SAz-2 sample with various exchangeable cations at EI-110CyH-SIH points and in the Mg-SAz-2 sample at
1001 EI-xCyH-SIH points.

Time of isothermal drying (h)	Interlayer cation					
	Mg	Mg	Mg	Ca	Na	Cs
	Temperature of isothermal segment					
	110 °C	200 °C	300 °C	110 °C	110 °C	110 °C
4	3.2	1.6	0.7	1.3	0.8	0.5
6	2.9	1.5	0.6	1.3	0.8	0.5
12	2.8	1.4	0.5	1.3	0.8	0.5

1002

1003

1004 Table 3. TBW contents in wt% from xC4H-SIH and xC-MIH experiments Negative values indicate reached onset of dehydroxylation.

Interlayer cation	Temperature of isothermal segment (°C)	Experiment type									
		SIH					MIH				
		Sample									
		SAP	SAz-2	SCa-3	SWy-2	SWa-1	SAP	SAz-2	SCa-3	SWy-2	SWa-1
Mg	110	4.1	3.2	2.6	2.8	1.6	4.3	2.8	2.4	2.5	3.0
	200	2.4	1.7	1.3	1.7	1.0	2.4	1.4	1.1	1.7	1.7
	300	1.6	0.8	0.3	0.7	-1.3	1.7	0.4	0.0	0.7	-1.5
Ca	110	1.2	1.6	1.4	1.6	1.1	1.6	1.4	1.3	1.9	1.9
	200	1.0	0.8	0.9	1.4	1.1	1.2	0.9	0.8	1.3	1.1
	300	0.6	0.3	0.2	0.6	-1.3	0.8	0.3	0.1	0.5	-1.6
Na	110	1.1	1.0	1.0	1.0	0.8	1.4	1.0	0.8	1.6	n.a.
	200	1.3	0.5	0.7	1.2	n.a.	1.0	0.7	0.5	1.3	n.a.
	300	0.7	0.1	0.2	0.6	n.a.	0.5	0.3	0.1	0.4	n.a.
Cs	110	0.6	1.0	1.1	0.6	0.4	0.7	0.9	0.5	0.7	2.3
	200	0.4	0.3	0.4	0.7	0.4	0.5	0.6	0.3	0.6	1.4
	300	0.7	0.0	0.1	0.3	-2.2	0.3	0.2	0.0	0.3	-1.5

1005 n.a. – not analyzed.

1006

1007

1008 Table 4. Temperatures of virtual onset of dehydroxylation (TVD; in °C) for SIH and MIH experiments, and corresponding temperatures of
1009 maximum of dehydroxylation rate (TDX; in °C).

	TDX (°C)																TVD Average (°C)	1σ	TDX Average (°C)	1σ
Experiment type	SIH												MIH							
Interlayer cation	Mg			Ca			Na			Cs			Mg	Ca	Na	Cs				
T of isothermal segment (°C)	110	200	300	110	200	300	110	200	300	110	200	300								
SAP	573	560	561	525	570	561	474	562	574	547	560	629	562	567	549	566	559	31	789	37
SAz-2	434	448	449	421	399	408	411	385	388	425	376	329	409	404	413	407	407	29	603	13
SCa-3	384	387	392	397	400	392	402	409	404	412	387	381	345	385	385	346	388	19	587	6
SWy-2	455	460	456	420	439	456	428	443	487	392	452	444	443	444	462	443	445	21	632	22
SWa-1	304	324	DX	306	324	DX	291	n.a.	n.a.	250	296	DX	DX	DX	n.a.	DX	299	25	386	32

1010 DX stands for dehydroxylation; n.a. – not analyzed

1011

This is a preprint, the final version is subject to change, of the American Mineralogist (MSA)
Cite as Authors (Year) Title. American Mineralogist, in press.
(DOI will not work until issue is live.) DOI: http://dx.doi.org/10.2138/am-2017-5918

1012 Table 5. TBW content in wt% for zeolites in SIH experiments.

Temperature of isothermal segment (°C)	Exchangeable cation	4A	1013 13X
110	Ca	6.2	5.0
	Na	4.0	4.3
200	Ca	3.4	2.8
	Na	2.6	1.7
300	Ca	1.9	1.2
	Na	0.6	0.8

1014

1015

1016

1017 Table 6. Activation energy (E_a) values of smectite dehydration and dehydroxylation from literature and the present study. See the text for details.

Dehydration[a]					
Sample	E_a (kJ/mol)		Experiment type and calculation method	Reference	Comments on the method of WBW and TBW assignment
	WBW or equivalent	TBW or equivalent			
Mg-Wyoming bentonite	35	121	TG, novel non-isothermal single-run method	Poinsignon et al. (1982)	Two dehydration stages above and below 100 °C
Ca-Wyoming bentonite	37	185			
Na-Wyoming bentonite	73	-			
K-Wyoming bentonite	79	-			
8 natural, predominantly Ca smectites	47-73		TG (non-isothermal), model fitting	Girgis et al. (1987)	Results representing mixed ranges for both TBW and WBW
Ca-mtm	33.5	47+/-6	TG (isothermal), model fitting	Bray and Redfern (1999)	Two dehydration stages above and below 90 °C,
Mg-Wyoming mtm	38	46	TG (non-isothermal), model fitting	Zabat and Van Damme (2000)	Two dehydration stages above and below 100 °C
Ca-Wyoming mtm	71	91			
Na-Wyoming mtm	42	-			
Cs-Wyoming mtm	54	-			
Ca-SWy-1	84(2)	127(5)	XRD pattern modeling	Ferrage (2007b)	WBW - transision between 2 and 1 water layers TBW - transition between 1 and 0 water layers
Na-mtm	68	-	TG (non-isothermal)	Prado and Vyazovkin	Dehydration below

			isoconversional	(2011)	100°C
Mg-SCa-3	-	88-161	TG (non-isothermal) isoconversional	This study[b]	
Ca-SCa-3	48+/-1	102-189			
Na-SCa-3	49+/-1	87-185			
Mg-SAz-2	-	76-139			
Ca-SAz-2	52+/-3	-			
Na-SAz-2	53+/-8	-			
Ca-SWy-2	45+/-1	-			
Na-SWy-2	47+/-1	-			
Dehydroxylation					
Mg- Wyoming mtm	175+/-20		TG (isothermal), model fitting	Bray and Redfern (2000)	
Ca-Wyoming mtm	261+/-22				
Na- Wyoming mtm	251+/-17				
K- Wyoming mtm	254+/-8				
Mg-SCa-3	219		TG (non-isothermal) isoconversional	This study	
Ca-SCa-3	238				
Na-SCa-3	231+/-2				
Cs-SCa-3	236+/-1				
Mg-SAz-2	159				
Ca-Saz-2	216+/-5				
Na-SAz-2	234				
Cs-Saz-2	249+/-2				

[a] E_a values from literature may not strictly correspond to distinction between WBW and TBW used in the present work. See the text for details.
[b] E_a of WBW removal from experiments without isothermal heating segment, E_a of TBW removal from experiments with isothermal heating segment.